Rate Allocation for Quantized Control Over Binary Symmetric Channels

Lei Bao, *Member, IEEE*, Mikael Skoglund, *Senior Member, IEEE*, Carlo Fischione, *Member, IEEE*, and Karl Henrik Johansson, *Senior Member, IEEE*

***Abstract*—Utility maximization in networked control systems (NCSs) is difficult in the presence of limited sensing and communication resources. In this paper, a new communication rate optimization method for state feedback control over a noisy channel is proposed. Linear dynamic systems with quantization errors, limited transmission rate, and noisy communication channels are considered. The most challenging part of the optimization is that no closed-form expressions are available for assessing the performance and the optimization problem is nonconvex. The proposed method consists of two steps: (i) the overall NCS performance measure is expressed as a function of rates at all time instants by means of high-rate quantization theory, and (ii) a constrained optimization problem to minimize a weighted quadratic objective function is solved. The proposed method is applied to the problem of state feedback control and the problem of state estimation. Monte Carlo simulations illustrate the performance of the proposed rate allocation. It is shown numerically that the proposed method has better performance when compared to arbitrarily selected rate allocations. Also, it is shown that in certain cases nonuniform rate allocation can outperform the uniform rate allocation, which is commonly considered in quantized control systems, for feedback control over noisy channels.**

***Index Terms*—Constrained nonconvex optimization, linear quadratic cost, quantized feedback control, rate allocation, utility maximization.**

I. Introduction

NETWORKED control systems based on limited sensor and actuator information have attracted increasing attention during the past decades [1], [2]. In future NCSs, monitoring and control tasks could be performed by simple, inexpensive, and small sensor nodes, which means that the transmitting and the computing resources are highly limited. After the deployment, it may not be possible to maintain or recharge the network and its nodes manually for reasons such as the physical location of the network, or harsh environment conditions. A major challenge is to design a sustainable network that is highly energy efficient, since the life time of such a network is determined by battery-powered devices.

The natural resources that govern digital radio communications are energy/power and bandwidth, and it is well known that power and bandwidth can be traded against each-other. In energy-critical applications, as in wireless sensor and actuator networks, it is fair to assume that radio nodes are operating in the power-efficient, wideband, regime, resulting in a direct (linear) connection between the transmission rate and the required energy per bit [3]. Hence, in such systems, being in the focus of this paper, using the available rate efficiently will have direct impact on the energy consumption. In general, increasing the transmission rate will always lead to higher cost of transmission, in terms of energy/power or bandwidth, or both. At this background, we focus on *efficient use of a limited bit-budget in quantized feedback control*. To reduce the rate, we study the case where the sensed data is quantized by using only a few bits per sample. In addition to lowering the cost of communication, there is also another important advantage in constraining the bit resolution per transmission, that of reducing the latency in the decoding. At low rates, and with a latency constraint in the decoding processing, channel errors cannot be prevented (since perfect error correction in general requires very long codewords, increasing the decoding delay). Furthermore, spending fewer bits on quantization will increase the quantization distortion. Designing schemes that efficiently carry out the joint action of quantization, channel protection and control is therefore of great importance.

Optimizing encoder-controller design is a challenging task, *cf.*, [5], [6]. On the other hand, from the practical point of view it is often of interest to use simple coding-control policies subject to satisfactory performance. Rate allocation can then be used to improve upon the system performance by exploiting the additional degree of freedom offered by communication resources. In general, one main obstacle to optimize the rates is the lack of tractable distortion functions, which model the performance index of the feedback control system. The optimization problem often becomes nonconvex, which implies that it is difficult to compute the optimal solution.

A. Related Work

Rate optimization for NCSs is a resource allocation problem where the utility function is expressed in terms of control performance. There is a vast literature on utility maximization with communication resource constraints [7]–[11]. However, expressing a utility function for NCSs introduces major challenges with respect to existing methods from the literature,

Manuscript received August 17, 2011; revised December 17, 2011; accepted February 01, 2012. Date of publication February 20, 2012; date of current version May 11, 2012. The associate editor coordinating the review of this manuscript and approving it for publication was Dr. Mathini Sellathurai. This work was supported in part by the EU project FeedNetBack, the EU project Hydrobionets, the Swedish Research Council, the Swedish Strategic Research Foundation, and the Swedish Governmental Agency for Innovation System.

L. Bao was with the Royal Institute of Technology (KTH) Electrical Engineering and ACCESS Linnaeus Centre, SE-10044 Stockholm, Sweden. She is now with Ericsson Research, SE-431 84 Mölndal, Sweden (e-mail: lei.bao@ee.kth.se; lei.bao@ericsson.se).

M. Skoglund, C. Fischione, and K. H. Johansson are with the KTH Electrical Engineering and the ACCESS Linnaeus Centre, SE-10044 Stockholm, Sweden (e-mail: skoglund@ee.kth.se; carlofi@ee.kth.se; kallej@ee.kth.se).

Color versions of one or more of the figures in this paper are available online at http://ieeexplore.ieee.org.

Digital Object Identifier 10.1109/TSP.2012.2188521

because of the presence of quantization errors, channel losses, and their impact on the control decisions, as we discuss next.

Allocating communication resources over space and time is important. For feedback control systems this is largely an open problem. Approaches to assigning bits among the elements of the state of the plant, while imposing a constraint on the number of transmitted bits over time, can be found in, e.g., [12] and [13]. In these works, it has been often assumed that bits (rates) are distributed to sensor measurements evenly over time. Owing to the nonstationarity of the state observations, an even distribution of bits over time to sensor measurements may not be efficient for networked control. It is natural to expect considerable gains by employing a nonuniform allocation of rates. Hence, optimizing the rate allocation is vital to overcome the limited communication resources and to achieve a better overall control and communication performance.

The rate allocation problem studied in this paper is related to classical rate allocation problems in communications, e.g., [14] and [15]. In these works, high-rate quantization theory is used to quantify the relation between rate and performance for a general class of quantizers. There exists a rich body of literature on the high-rate analysis of quantized system, for both noiseless and noisy communication channels [16]–[18]. It is worth remarking that although high-rate theory requires high rates to be perfectly valid, this theory can often be used at a lower rate [19]. Experience has shown that high-rate theory can also make useful predictions at low rate which is the case in this paper. Further, previous work on rate allocation has often focused on the special case of optimized quantizers, for example in [20] the optimal quantizer is studied in the context of transform codes, where the distortion introduced by the quantizer is a convex function, and a closed-form optimal solution can be derived. However, in our setting we will show that the overall distortion is a nonconvex function of the instantaneous rates, which makes more difficult the computation of the optimal solution.

Quantization and transmission errors are crucial obstacles to maximize the control system performance. The quantization deteriorates the signals transmitted between the plant and the controller, which can potentially degrade the overall control system performance substantially. In the literature, quantization errors have mainly been modeled as additive white Gaussian noise [14], [21], uncorrelated with the signal being quantized. The advantage of this model is that many tools and methods can be readily applied. In the beginning of the 1990's, research interest in the stability analysis of quantized control systems was triggered by [22]. In that paper the author showed that, even for the simplest dynamic system (linear, scalar and noiseless), it is not possible to stabilize an unstable plant asymptotically with a static controller of a finite data rate. Since then, a wide range of interesting problems have been formulated and studied. The properties of static quantizers are thoroughly studied in, e.g., [22] and [23]. For this type of quantizers, the classical notion of stability is no longer relevant. Instead, attractivity and practical stability are introduced. Unlike the case of static quantizers, asymptotic stability is possible when time-varying quantizers are used, e.g., [12], [24]. Asymptotic stability is achieved by employing a "zooming"-strategy in [25]. The basic idea is that the quantizer resolution is increased when the state is close to the equilibrium, while the resolution is reduced when the state is far away. The fundamental problem of the minimum data rate required to asymptotically stabilize an unstable plant was studied in, e.g., [24], [26]–[28]. In the aforementioned works, the communication channel was essentially assumed to be noise-free, and the only limitation imposed by the channel is the limited data rate. Some recent works on control over a *noisy channel* include [27], [29]–[32]. Most work on control with limited information has been devoted to stability issues, while optimal designs are much less explored in the literature. Exceptions include the study of optimal stochastic control over communication channels, e.g., [5], [6], [28], [33]. Including the topic of control over rate-limited communication channel, the special issue on technology of networked control system [34] and the survey [35] provide excellent overview of a number of important communication and control challenges and recent results in the field of control over communication networks.

B. Contributions and Organization

The main contribution of this paper is a novel method for rate allocation for state feedback control of a linear system over a noisy channel. Specifically, we are interested in the optimization of two important cases of closed-loop control under communication constraints: linear feedback control and state estimation. By resorting to an approximation based on high-rate quantization theory, we are able to derive a computationally feasible scheme that seeks to minimize the overall distortion over a finite time horizon. The resulting rate allocation is not necessarily evenly distributed, as opposed to what is commonly assumed in the literature aforementioned. Overall good performance of our method is shown by numerical simulations. The goal of the paper is to demonstrate how rate allocation can be used to improve the overall performance of a control system, subject to given types of encoders and controllers. The proposed scheme is applicable for a general class of quantizers to meet requirements of different applications.

The remaining part of this paper is organized as follows. In Section II, the control system is described and the rate allocation problem is formulated. A brief review on some useful results of high-rate quantization theory is included in Section III. Thereafter, the rate allocation problems for linear feedback control, as well as state estimation, are solved in Section IV. Numerical simulations are carried out in Section V to demonstrate the performance of the proposed rate allocation method.

Notation

Let $\mathbb{R}$, $\mathbb{N}$ and $\mathbb{Z}^+$ denote the sets of real numbers, natural numbers and nonnegative integers, respectively. We use $\mathbf{E}\{\cdot\}$ to denote the expectation operator, and $(\cdot)'$ the matrix transpose. An optimal solution is denoted by $(\cdot)^\star$. Moreover, $p(\cdot)$ denotes a probability density function (pdf) and $\Pr(\cdot)$ denotes a probability.

II. System Description and Problem Statement

The goal of this paper is to arrive at a new rate allocation method for state feedback control over a noisy channel. Fig. 1 shows a block-diagram of the control system we investigate. First, we briefly introduce each building block of the system, and then describe the rate constrained optimization problem.

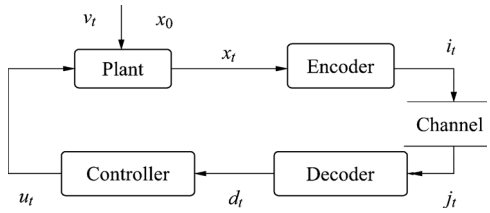

Fig. 1. Block-diagram for the closed-loop system studied in this paper. The system has a separate decoder unit and a controller. This paper aims at demonstrating that rate allocation can improve significantly the performance of the control.

Finally, the coding unit and the channel will be explained in more detail.

A. System Description

Throughout this paper we consider a scalar system where the plant is governed by the linear equation

$$x_{t+1} = ax_t + u_t + v_t \tag{1}$$

where $x_t, u_t, v_t \in \mathbb{R}$, are the state, the control and the process noise, respectively. Process noise v_t is modeled as a white Gaussian noise sequence of variance σ_v^2, i.e., $v_t \sim \mathrm{N}(0, \sigma_v^2)$. It is mutually independent of the initial state x_0, which is also assumed to be zero-mean Gaussian, $x_0 \sim \mathrm{N}(0, \sigma_{x_0}^2)$. Since the focus of the paper is on the optimization of the overall system performance, we assume that the open-loop system is stable, i.e., $|a| \leq 1$. Nevertheless, communication errors might degrade the system performance significantly, even destabilize an open-loop stable system. For analytical simplicity, we also assume that the state is available at the encoder, although a state measurement with measurement error can be included easily at the cost of more complex notation and derivations. More details for such an extension and the multidimensional case can be found in [36].

At the encoder, the full state measurement is coded by a memoryless time-varying encoder, which takes the current state x_t as the input, and produces an index i_t

$$i_t = f_t(x_t, R_t) \tag{2}$$

where the time-varying instantaneous rate $R_t \in \mathbb{Z}^+$ is to be determined later. Note that the encoder can be adapted to the statistical time variation of the state x_t and depends on R_t. We introduce the index set $\mathcal{L}_t(R_t) = \{0, \ldots, 2^{R_t} - 1\} \subseteq \mathbb{Z}^+$, and for a given R_t, $i_t \in \mathcal{L}_t$.

The index i_t will be mapped into a binary codeword before being fed to a binary channel. As commented in Section I, since closed-loop control is a time-critical application, we cannot use long codewords to prevent channel transmission errors. Hence, the binary channel codewords assumed here do not introduce additional redundancy, i.e., each member of $\mathcal{L}_t(R_t)$ is mapped to a codeword of length R_t. Such a mapping from an index to a codeword is commonly referred to as the index assignment (IA). Unlike in the error-free scenarios where all IA's perform equally well, in the presence of channel errors different IA's have different impact on the system performance. Finding the optimal IA is a combinatorial problem which is known to be NP-hard [37]. Therefore, in this paper we average out the dependence on a specific IA by randomization. At each transmission, a random assignment is generated and revealed to the encoder and decoder. Previous work that assumed a random IA to facilitate further analysis includes, e.g., [18] and [38]. Assigning a new IA randomly for each transmission is impractical in real communication systems. However, using the random IA in the analysis can characterize the average performance for a given rate allocation, and one can always find at least one IA which performs at least as well as the average over the random assignments (cf., random coding arguments in information theory [39]). It is possible to find a variety of IA's which outperform the random assignment. In practice, we can first use random IA in the analysis to optimize the rate allocation. For the optimized rate allocation we can adopt an IA which performs better than the random assignment.

The overall channel, composed by the combination of the random index assignment and a binary symmetric channel (BSC), is completely specified by the symbol transition probabilities $\Pr(j_t|i_t)$, with $j_t \in \mathcal{L}_t$ denoting the received index. At the bit level, the channel is characterized by the crossover probability of the BSC, $\epsilon = \Pr(0|1) = \Pr(1|0)$. Because of the symmetry, it is reasonable to consider $0 \leq \epsilon \leq 0.5$. The overall symbol error probability $\Pr(j_t|i_t)$ is determined by both ϵ and the randomized IA, according to

$$\Pr(j_t|i_t) = \begin{cases} \alpha(R_t), & j_t \neq i_t, \\ 1 - (2^{R_t} - 1)\alpha(R_t), & j_t = i_t, \end{cases} \tag{3}$$

where $\alpha(R_t) \triangleq \frac{(1-(1-\epsilon)^{R_t})}{(2^{R_t}-1)}$ is obtained by averaging over all possible IA's [38]. For this channel, all symbol errors are equally probable.

At the receiver side, there is a separate decoder unit and a controller. The decoder takes the instantaneous channel output j_t as the input, and produces an estimate of x_t, denoted by d_t,

$$d_t = D_t(j_t) \in \mathbb{R} \tag{4}$$

where $D_t(\cdot)$ is an arbitrary deterministic function. The estimate d_t can take on one of 2^{R_t} values, referred to as the reconstructions. Finally, the control u_t is computed based on the decoded symbol, $u_t = g_t(d_t) \in \mathbb{R}$. We will be more specific about the control function $g_t(\cdot)$ after the rate allocation problem is presented.

We remark here that memoryless encoder-controller mappings are considered in the paper mainly because they are practical, and also, the aim of the paper is to demonstrate the basic concept that rate allocation can be used to improve the overall performance of a control system. The optimization in this paper is performed with respect to the transmission rate, subject to given types of encoders and controllers, as described in the next subsection. The rate allocation technique we investigate is applicable to a wide range of encoder-controller mappings, including the optimal mappings. Regarding real applications, it is often of practical interest to implement simple encoders and controllers with satisfactory performance. Optimizing rate allocation for simple coding-control policies may be more realistic than optimizing fixed-rate encoder-controller mappings.

Moreover, our proposed rate allocation techniques can be applied to encoders and controllers with memory. In general, the overall system performance can be improved by having access

to past information. However, in the presence of process noise, the significance of memory is often limited. Due to the unreliable communications between the encoder and controller, the uncertainty in the memory should be addressed. A common solution is to introduce side-information to the system to inform the encoder about the channel outputs. For the purpose of rate allocation, there is no essential difference, besides the increased complexity of the system and computational burden.

Our problem could be viewed as one of the two subproblems of the general problem that the transmission rate and encoder-controller mappings are optimized jointly. By specifying the type of encoder-controller, we have imposed a certain structure on the coding-control mappings. Compared with the general problem, our problem is still a challenge in its own right. The other subproblem is the optimization of fixed-rate coding-control mappings, *cf.*, [5] and [6].

B. Problem Statement

The control objective is to minimize the expected overall cost $\mathbf{E}\{J_{\rm tot}(\mathbf{R})\}, \mathbf{R}=\{R_0,\ldots,R_{T-1}\}$, over a finite horizon, subject to a rate constraint $\sum_{t=0}^{T-1} R_t \le R_{\rm tot}, R_t \in \mathbb{Z}^+$, with $R_{\rm tot}$ denoting the total rate. We motivated this constraint in Section I, noting that increasing the rate will always lead to higher cost of communication in general, and increased energy consumption in particular. Also, since we assume that the individual rates, R_t, are typically very low, it is important to allocate each available bit wisely. The constraint is typical of water-filling resource allocation [40], [41]. We refer to the whole sequence $\mathbf{R}$ as the bit-rate allocation. Throughout this paper, we say "for all t" when we mean "for $t=0,\ldots,T-1$".

Next, we introduce an objective function which we will use to describe both the state feedback control problem and the state estimation problem. More specifically, $J_{\rm tot}(\mathbf{R})$ is the quadratic function

$$J_{\rm tot}(\mathbf{R})=\sum_{t=0}^{T-1} J_t(\mathbf{R}_t)=\sum_{t=0}^{T-1}\psi_t(x_t-d_t)^2,\ \psi_t>0 \qquad (5)$$

where $J_t(\mathbf{R}_t)$ denotes the instantaneous objective function, $\mathbf{R}_t=\{R_0,\ldots,R_t\}$, and $\psi_t, t=1\ldots T-1$, are positive constants. In the remaining part of this subsection we use (5) to formulate rate allocation problems for state feedback control and state estimation.

First, we formulate the problem of rate allocation for state feedback control, where we consider to minimize the expected value of the quadratic function

$$J_{\rm tot}(\mathbf{R})=\sum_{t=0}^{T-1} J_t(\mathbf{R}_t)=\sum_{t=1}^{T} x_t^2+\rho u_{t-1}^2 \qquad (6)$$

where $\rho \ge 0$ is the weighting factor. The function (6) is the linear quadratic (LQ) cost from classical stochastic control [42]. The aim of using (6) is to minimize the state variance at all time instances, with a power constraint on the control signal. The relation between the rate allocation $\mathbf{R}$ and the cost $\mathbf{E}\{J_{\rm tot}(\mathbf{R})\}$ depends on the channel and the coding-control scheme, which will be specified next.

From classical linear quadratic control theory we know that because the process noise v_t is white, uncorrelated with x_t and u_t, we can write $\mathbf{E}\{J_{\rm tot}(\mathbf{R})\}$, with $J_{\rm tot}(\mathbf{R})$ given by (6), as

$$\mathbf{E}\{J_{\rm tot}(\mathbf{R})\}=\mathbf{E}\left\{(\phi_0-1)x_0^2+\sum_{t=0}^{T-1}\phi_{t+1}v_t^2 + \sum_{t=0}^{T-1}(\phi_{t+1}+\rho)(-x_t\ell_t+u_t)^2\right\}, \qquad (7)$$

where ϕ_t and ℓ_t are defined as

$$\phi_t \triangleq 1+\frac{a^2\phi_{t+1}\rho}{\phi_{t+1}+\rho},\ \phi_T=1, \qquad (8)$$

$$\ell_t \triangleq -\frac{a\phi_{t+1}}{\phi_{t+1}+\rho}. \qquad (9)$$

Clearly, only the terms in the last sum of (7) are affected by control. According to classical linear quadratic Gaussian (LQG) theory [42], when the channel imperfections are absent (no quantization distortion and transmission error), the optimal control is given by $u_t=\ell_t x_t$. If the estimate d_t is close to the true state x_t then the classical LQG controller, which is a suboptimal solution in the presence of communication channels, is expected to give good results, even though it does not account for channel errors and quantization distortion. Motivated by the importance of classical LQG theory, in this paper we focus on the linear control policy

$$u_t=\ell_t d_t \qquad (10)$$

where ℓ_t is calculated according to (8). By using(10), minimizing $\mathbf{E}\{J_{\rm tot}(\mathbf{R})\}$ of (6) is equivalent to minimizing the expected value of

$$J_{\rm tot}(\mathbf{R})=\sum_{t=0}^{T-1}\pi_t(x_t-d_t)^2 \qquad (11)$$

where π_t is defined as

$$\pi_t \triangleq (\phi_{t+1}+\rho)\ell_t^2\,. \qquad (12)$$

Hence, the objective function (11) is equal to (5) with $\psi_t=\pi_t$. Therefore, for state feedback control we replace the objective function (6) with (11), and the new instantaneous objective function is

$$\mathbf{E}\{J_t(\mathbf{R}_t)\}=\pi_t\mathbf{E}\left\{(x_t-d_t)^2\right\}. \qquad (13)$$

Summarizing the above discussions, Problem 1 below specifies the rate allocation problem for state feedback control studied in this paper.

Problem 1: Given a linear plant of (1), a discrete memoryless channel of (3), a memoryless encoder-decoder pair of (2) and (4), subject to the linear control law (10), find the optimal bit-rate allocation $\mathbf{R}$ which minimizes the expected objective function (6), subject to the total bit constraint, i.e.,

$$\min_{\mathbf{R}}\ \sum_{t=0}^{T-1}\pi_t\mathbf{E}\left\{(x_t-d_t)^2\right\},\ \text{s.t.}\sum_{t=0}^{T-1}R_t\le R_{\rm tot},\ R_t\in\mathbb{Z}^+,\forall t.$$

A special case of the linear feedback control problem is the state estimation problem. Consider the case of the system (1) when $u_t = 0$, and the dynamic system is governed by

$$x_{t+1} = ax_t + v_t,\ a > 0. \tag{14}$$

Then, the expected state estimation error is

$$J_{\text{tot}}(\mathbf{R}) = \sum_{t=0}^{T-1} (x_t - d_t)^2 \tag{15}$$

where $\psi_t = 1$. We summarize the state estimation problem as follows.

Problem 2: Given a linear plant of (14), a discrete memoryless channel of (3), a memoryless encoder-decoder pair of (2) and (4), find the rate allocation $\mathbf{R}$ that solves the problem,

$$\min_{\mathbf{R}} \sum_{t=0}^{T-1} \mathbf{E}\left\{(x_t - d_t)^2\right\},\ \text{s.t.} \sum_{t=0}^{T-1} R_t \le R_{\text{tot}},\ R_t \in \mathbb{Z}^+,\ \forall t.$$

In striving to solve Problem 1 and Problem 2, there are two major difficulties. First, they are integer programming problems which are hard to solve because of the computational complexity. In this paper, we apply the classical approach [14] that first the rate allocation is optimized by relaxing the nonnegativity and integer constraints. Thereafter these constraints are dealt with by rounding. Second, the problems require the characterization of the mean squared error (MSE) $\mathbf{E}\left\{(x_t - d_t)^2\right\}$ as a function of the instantaneous rates, which does not have an analytical explicit expression in general. We simplify this problem by introducing two approximations: the high rate approximation of the reconstructions and the Gaussian approximation of the state x_t. As a result, we are able to write the overall cost in terms of all previous rate, and moreover, strong duality applies to the constrained optimization problem, as shown in Section IV. Next, we address the high-rate approximation of MSE in Section III. Then later in Section IV, we describe the Gaussian approximation of the state in the control system.

III. High-Rate Approximation of MSE

We have seen in the previous section that the MSE $\mathbf{E}\left\{(x_t - d_t)^2\right\}$ appears to be a central figure-of-merit both in the state feedback control problem and the state estimation problem. In general, it is hard to formulate closed-form expressions for the MSE, even in the case of simple uniform quantizers. We have to resort to approximations. Inspired by the classical works on rate allocation in communications, e.g., [14], we resort to high-rate quantization to compute MSE. For general aspects about high-rate quantization theory, we refer the reader to, e.g., [18] and [38].

Given that it is impossible to formulate a closed-form expression for the MSE, we show a useful approximation derived under the high-rate assumption. Roughly speaking, the high-rate assumption requires that the pdf of the source is approximately constant within the same quantization cell. Following [18], in case of the symmetric channel (3), a high-rate approximation of the MSE is

$$\mathbf{E}\left\{(x_t - d_t)^2\right\} \approx 2^{R_t}\alpha(R_t)\sigma_{x_t}^2 + \varphi_t\alpha(R_t) \times \int_{y\in\mathbb{R}} y^2\lambda_t(y)\mathrm{d}y + \frac{G^{-2}}{3}\varphi_t^{-2}\int_{x\in\mathbb{R}} \lambda_t^{-2}(x)p(x_t = x)\mathrm{d}x,$$

where the source x_t is zero-mean with variance $\sigma_{x_t}^2$, and $p(x_t = x)$ denotes the probability density function of x_t. Further, in (16), the constant G represents the volume of a unit sphere, and for a scalar quantizer $G = 2$. The function $\lambda_t(x)$ is referred to as the point density function [18], specifying the density of the (arbitrary) reconstruction d_t. Resembling a probability density function, it follows that $\lambda_t(x) \ge 0$, for all x_t, and $\int_{\mathbb{R}} \lambda_t(x)\mathrm{d}x = 1$. Finally, the parameter φ_t, $1 \le \varphi_t \le 2^{R_t}$, specifies the number of codewords the encoder will chose. If the crossover probability ϵ is large, then in order to protect against the channel error, a good encoder may only use a part of the available codewords. For simplicity, we assume $\varphi_t = 2^{R_t}$, throughout this paper.

Essentially, we are interested in an efficient approximation to describe the relation between the MSE and the rate R_t. By a further approximation, $2^{R_t}\alpha(R_t) \approx 1 - (1-\epsilon)^{R_t}$, we rewrite (16) and introduce the high-rate approximation $\hat{\mathrm{J}}_t$

$$\begin{aligned}\mathbf{E}\left\{(x_t - d_t)^2\right\} &\approx \hat{\mathrm{J}}_t(\beta_t, \kappa_t, R_t) \triangleq \beta_t(1 - (1-\epsilon)^{R_t}) + \kappa_t 2^{-2R_t},\\ \beta_t &\triangleq \sigma_{x_t}^2 + \int_y y^2\lambda_t(y)\mathrm{d}y,\\ \kappa_t &\triangleq \bar{G}\int_x \lambda_t^{-2}(x)p(x_t = x)\mathrm{d}x,\end{aligned} \tag{16}$$

where $\bar{G} \triangleq \frac{G^{-2}}{3}$. For practical sources and encoder-decoder pairs, it follows that $0 < \beta_t < \infty$, and $0 < \kappa_t < \infty$, which is considered throughout this paper. The expression of the distortion $\hat{\mathrm{J}}_t$ in (16) is rather general for a large variety of quantizers, described by means of the point density function, and derived under the high-rate assumption. It could be observed that the crossover probability ϵ influences the convexity of the function. When $\epsilon = 0$, $\hat{\mathrm{J}}_t$ is monotonically decreasing in R_t. In fact, $\hat{\mathrm{J}}_t$ is a convex function in R_t. On the other hand, for noisy channels, convexity only applies for certain $\{\beta_t, \kappa_t\}$ pairs. For the general case of an arbitrary $\{\beta_t, \kappa_t\}$ pair, (16) is a quasi-convex function in R_t, as stated in Lemma 1.

Definition 1: Quasi-convex function [40] Let $domf$ be the domain of $f : \mathbb{R}^n \mapsto \mathbb{R}$. The function f is quasi-convex if its domain and all its sublevel sets $\mathcal{S}_\alpha = \{x \in domf : f(x) \le \alpha\}$, for $\alpha \in \mathbb{R}$, are convex.

Lemma 1: The distortion function $\hat{\mathrm{J}}_t(\beta_t, \kappa_t, R_t) = \beta_t(1 - (1-\epsilon)^{R_t}) + \kappa_t 2^{-2R_t}$, $0 < \beta_t < \infty$, $0 < \kappa_t < \infty$, is a quasi-convex function in the variable R_t and there is a unique global minimizer with respect to R_t.

Proof: The proof follows by taking the first- and second-order derivative of $\hat{\mathrm{J}}_t(\beta_t, \kappa_t, R_t)$. The first-order derivative is $\frac{\partial\hat{\mathrm{J}}_t}{\partial R_t} = -\beta_t \ln(1-\epsilon)(1-\epsilon)^{R_t} - 2\ln(2)\kappa_t 2^{-2R_t}$, and it has at most one critical point $R_t^\star$, which solves $-\beta_t \ln(1-\epsilon)(1-\epsilon)^{R_t^\star} - 2\ln(2)\kappa_t 2^{-2R_t^\star} = 0$. This is observed since the first term of the derivative, $-\beta_t \ln(1-\epsilon)(1-\epsilon)^{R_t}$, is strictly decreasing towards 0 as R_t grows, and the second term $-2\ln(2)\kappa_t 2^{-2R_t}$ is strictly increasing towards 0 as R_t grows. Note also, for $0 \le \epsilon \le 0.5$, $(1-\epsilon)^{R_t}$ decreases more slowly than 2^{-2R_t}. Thus, for all $R_t < R_t^\star$, $\frac{\partial\hat{\mathrm{J}}_t}{\partial R_t}$ is negative, and $\hat{\mathrm{J}}_t$ is monotonically decreasing; for all $R_t > R_t^\star$, $\frac{\partial\hat{\mathrm{J}}_t}{\partial R_t}$ is positive, and $\hat{\mathrm{J}}_t$ is monotonically increasing. In case that $\epsilon = 0$, the critical point is at $R_t^\star = \infty$, since $\lim_{R_t \to \infty} \frac{\partial\hat{\mathrm{J}}_t}{\partial R_t} = 0$. The second-order derivative is $\frac{\partial^2\hat{\mathrm{J}}_t}{\partial R_t^2} = -\beta_t \ln^2(1-\epsilon)(1-\epsilon)^{R_t} + 4\ln^2(2)\kappa_t 2^{-2R_t}$.

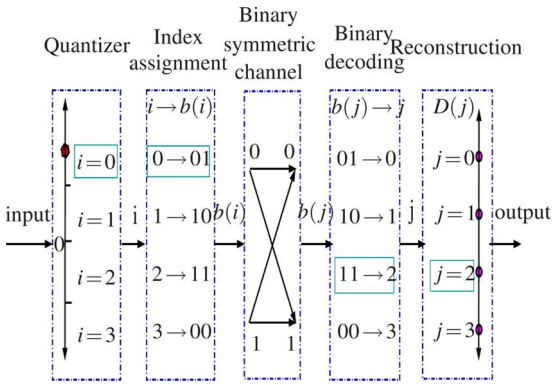

Fig. 2. A diagram of data transmission over a binary symmetric channel. As an example, the index $i = 0$ is mapped to the binary codeword 01, and the codeword 11 is received due to the error imposed by the channel. The decoded index is $j = 2$.

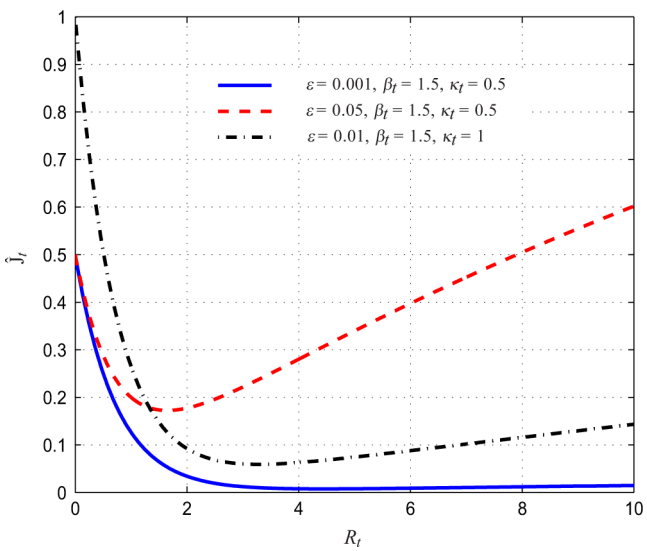

Fig. 3. The impact of R_t, κ_t, β_t, and ϵ on the objective function $\hat{\mathrm{J}}_t$.

The critical point is a global minimum, since the second-order derivative of the critical point is larger than 0. ■

In Fig. 3, some examples of $\hat{\mathrm{J}}_t$ are depicted to show the impact of the variables β_t, κ_t and R_t. Generally speaking, as the rate increases, the quantization distortion decreases, while the distortion caused by transmission errors grows. Beyond the critical point, the latter distortion dominates, and therefore the overall distortion will increase with the rate. Moreover, for the same quantizer, the higher the crossover probability ϵ, the closer to 0 the critical point is. As will be shown later, Lemma 1 is instrumental to solve the rate allocation problems studied in this paper. Here we introduce a class of $\hat{\mathrm{J}}_t$, which can be written as

$$\begin{aligned}\hat{\mathrm{J}}_t(\beta_t,\kappa_t,R_t) &= \sigma_x^2\tilde{\mathrm{J}}_t(\tilde{\beta}_t,\tilde{\kappa}_t,R_t)\\ &= \sigma_{x_t}^2\left(\tilde{\beta}_t(1-(1-\epsilon)^{R_t})+\tilde{\kappa}_t 2^{-2R_t}\right),\end{aligned} \quad (17)$$

i.e., $\beta_t = \sigma_x^2\tilde{\beta}_t$ and $\kappa_t = \sigma_x^2\tilde{\kappa}_t$, where $\tilde{\beta}_t > 0$ and $\tilde{\kappa}_t > 0$ are independent of R_t and $\sigma_{x_t}^2$. As shown later, this class of $\hat{\mathrm{J}}_t$ is central to our solutions to the state feedback control problems. Owing to the fact that $\tilde{\mathrm{J}}_t$ is a special case of $\hat{\mathrm{J}}_t$, Lemma 1 applies directly to $\tilde{\mathrm{J}}_t$. Finally, we use a uniform quantizer to illustrate the computation of $\hat{\mathrm{J}}_t$ according to (16) and (17).

Example 1: **Uniform quantizer and Gaussian source** Recall that throughout the paper, encoder-controller pairs are memoryless mappings and functionally equivalent to a quantizer. Owing to its simplicity, the uniform quantizer is thoroughly studied in the literature and widely used in practice. In the example, we describe the step length $\Delta_t = \frac{2\vartheta_t}{2^{R_t}}$ of a uniform quantizer as a function of the quantizer range $[-\vartheta_t, \vartheta_t]$ and the rate R_t. The quantizer works as follows,

$$i_t = \begin{cases} 0, & x_t < -\vartheta_t + \Delta_t,\\ k, & -\vartheta_t + k\Delta_t \le x_t \le -\vartheta_t + (k+1)\Delta_t,\ k \in \mathbb{N},\\ 2^{R_t}-1, & x_t > \vartheta_t - \Delta_t. \end{cases}$$

The parameter ϑ_t can be selected with respect to the source signal. Consider a source x_t, and let $p_{\vartheta_t} \triangleq \Pr(x_t \in [-\vartheta_t, \vartheta_t])$ denote the probability that x_t is within the range of the quantizer. If x_t is zero-mean Gaussian with variance $\sigma_{x_t}^2$, then ϑ_t is related to p_{ϑ_t} and σ_x^2 as $\vartheta_t = \sigma_{x_t} Q^{-1}\left(\frac{(1-p_{\vartheta_t})}{2}\right)$, where $Q^{-1}(\cdot)$ is the inverse of the Q-function, $Q(x) \triangleq \int_x^\infty \frac{1}{(\sqrt{2\pi})} e^{\frac{-y}{2}} \mathrm{d}y$.

For a uniform quantizer with a quantization range $[-\vartheta_t, \vartheta_t]$, the point density function is then $\lambda_t(x_t) = \frac{1}{(2\vartheta_t)}$. If the source signal and the uniform quantizer share the same range $[-\vartheta_t, \vartheta_t]$, then the high-rate approximation $\hat{\mathrm{J}}_t$, according to (16), is $\hat{\mathrm{J}}_t = \left(\sigma_{x_t}^2 + \frac{\vartheta_t^2}{3}\right)(1-(1-\epsilon)^{R_t}) + 4\vartheta_t^2\bar{G}2^{-2R_t}$, which means $\beta_t = \sigma_{x_t}^2 + \frac{\vartheta_t^2}{3}$ and $\kappa_t = 4\vartheta_t^2\bar{G}$. The first-order derivative of $\hat{\mathrm{J}}_t$, with respect to R_t, is $\frac{\partial \hat{\mathrm{J}}_t}{\partial R_t} = -\left(\sigma_{x_t}^2 + \frac{\vartheta_t^2}{3}\right)(1-\epsilon)^{R_t}\ln(1-\epsilon) - 8\vartheta_t^2\bar{G}2^{-2R_t}$. If the distortion caused by signals out of the quantizer support $[-\vartheta_t, \vartheta_t]$ is negligible, then a high-rate approximation of the MSE can be written as (17) with $\tilde{\beta}_t = 1 + \frac{\left(\left(Q^{-1}\left(\frac{(1-p_{\vartheta_t})}{2}\right)\right)^2\right)}{3}$ and $\tilde{\kappa}_t = 4\bar{G}\left(Q^{-1}\left(\frac{(1-p_{\vartheta_t})}{2}\right)\right)^2$.

IV. Rate Allocation

Now we are in the position to investigate the rate allocation problem for state feedback control. The essential challenge is that the communication between the sensor and the controller affects all future states. Estimating the key terms, such as $\mathbf{E}\{x_t^2\}$ and $\mathbf{E}\{(x_t - d_t)^2\}$, is a formidable task because the estimation error propagates with time in a highly non linear fashion. Therefore, we approximate the pdf of the state x_t by a zero-mean Gaussian function, since the initial state and the process noise are zero-mean Gaussian. By imposing the Gaussian approximation, we need only estimate the variance, with the estimated variance denoted by $\hat{\sigma}_{x_t}^2$. The next challenge lies in the derivation of $\hat{\sigma}_{x_t}^2$. We consider an upper bound for $\hat{\sigma}_{x_t}^2$ by simplifying the correlation between x_t and d_t, such that

$$\hat{\sigma}_{x_t}^2 = (A_t + B_t\tilde{\mathrm{J}}_{t-1}(\tilde{\beta}_{t-1}, \tilde{\kappa}_{t-1}, R_{t-1}))\hat{\sigma}_{x_{t-1}}^2 + \sigma_v^2 \quad (18)$$

where $A_t > 0$ and $B_t > 0$ are independent of R_{t-1}, $\hat{\sigma}_{x_{t-1}}^2$ and σ_v^2. The above assumption is reasonable, as illustrated by the following two cases.

Case 1: Consider the decoder $d_t = \mathbf{E}\{x_t | j_t\}$. In this case, the estimation error $x_t - d_t$ is uncorrelated with the estimate

d_t, so we can write $\mathbf{E}\left\{(x_t-d_t)^2\right\}=\mathbf{E}\left\{x_t^2\right\}-\mathbf{E}\left\{d_t^2\right\}$, and approximate $\mathbf{E}\left\{x_t^2\right\}$ as

$$\begin{aligned}\mathbf{E}\left\{x_t^2\right\}&=a^2\mathbf{E}\left\{x_{t-1}^2\right\}+\ell_{t-1}^2\mathbf{E}\left\{d_{t-1}^2\right\}\\&\quad+2a\ell_{t-1}\mathbf{E}\left\{x_{t-1}d_{t-1}\right\}+\sigma_v^2\\&\approx\Big(a^2+\ell_{t-1}^2+2a\ell_{t-1}-(\ell_{t-1}^2+2a\ell_{t-1})\\&\quad\times\tilde{\mathrm{J}}_{t-1}(\tilde{\beta}_{t-1},\tilde{\kappa}_{t-1},R_{t-1})\Big)\mathbf{E}\left\{x_{t-1}^2\right\}\\&\quad+\sigma_v^2,\end{aligned}\tag{19}$$

by using the high-rate approximation $\mathbf{E}\left\{(x_{t-1}-d_{t-1})^2\right\}\approx\mathbf{E}\left\{x_{t-1}^2\right\}\tilde{\mathrm{J}}_{t-1}(\tilde{\beta}_{t-1},\tilde{\kappa}_{t-1},R_{t-1})$. Hence, based on (19), we can relate the approximations $\hat{\sigma}_{x_t}^2$ and $\hat{\sigma}_{x_{t-1}}^2$ as

$$\begin{aligned}\hat{\sigma}_{x_t}^2=\Big(&a^2+\ell_{t-1}^2+2a\ell_{t-1}-(\ell_{t-1}^2+2a\ell_{t-1})\tilde{\mathrm{J}}_{t-1}\\&\times(\tilde{\beta}_{t-1},\tilde{\kappa}_{t-1},R_{t-1})\Big)\hat{\sigma}_{x_{t-1}}^2+\sigma_v^2,\end{aligned}$$

which corresponds to (18), with

$$A_t=a^2+\ell_{t-1}^2+2a\ell_{t-1},\ B_t=-(\ell_{t-1}^2+2a\ell_{t-1}).\tag{20}$$

In general, we can write $\mathbf{E}\left\{x_t^2\right\}$ as,

$$\begin{aligned}\mathbf{E}\left\{x_t^2\right\}&=\ell_{t-1}^2\mathbf{E}\left\{(x_{t-1}-d_{t-1})^2\right\}\\&\quad+(a+\ell_{t-1})^2\mathbf{E}\left\{x_{t-1}^2\right\}-2(a+\ell_t)\ell_t\\&\quad\times\mathbf{E}\left\{x_{t-1}(x_{t-1}-d_{t-1})\right\}+\sigma_v^2.\end{aligned}\tag{21}$$

The term $\mathbf{E}\left\{x_{t-1}(x_{t-1}-d_{t-1})\right\}$ depends on the source, quantizer and channel, and therefore it is often hard to formulate a closed-form expression. Below we show another case when (18) applies.

Case 2: Consider the case that $\mathbf{E}\left\{x_{t-1}(x_{t-1}-d_{t-1})\right\}$ in (21) can be written as a linear function of $\mathbf{E}\left\{x_{t-1}^2\right\}$, such as $\mathbf{E}\left\{x_{t-1}(x_{t-1}-d_{t-1})\right\}=\Gamma(\epsilon)\mathbf{E}\left\{x_{t-1}^2\right\}$, where Γ depends only on ϵ. Utilizing this linear relation together with the high-rate approximation, $\hat{\sigma}_{x_t}^2$ can be expressed in (18), with

$$A_t=(a+\ell_{t-1})^2-2(a+\ell_{t-1})\ell_{t-1}\Gamma(\epsilon),\ B_t=\ell_{t-1}^2.\tag{22}$$

Based on (16) and (18), an approximation of the instantaneous objective function (13) is given by

$$\begin{aligned}\mathbf{E}\left\{J_t(\mathbf{R}_t)\right\}&\approx\breve{J}_t(\mathbf{R}_t)\triangleq(\phi_{t+1}+\rho)\ell_t^2\hat{\sigma}_{x_t}^2\tilde{\mathrm{J}}_t(\tilde{\beta}_t,\tilde{\kappa}_t,R_t)\\&=\pi_t\hat{\sigma}_{x_t}^2\tilde{\mathrm{J}}_t(\tilde{\beta}_t,\tilde{\kappa}_t,R_t).\end{aligned}\tag{23}$$

where $\hat{\sigma}_{x_t}^2$ follows (18). In practice, the approximation (23) can be applied generally to all systems from Section II-B by finding suitable A_t and B_t to approximate the true objective functions.

As explained earlier that the rate R_t is a nonnegative integer number, therefore, we will first solve a relaxed problem by optimizing rate allocation for $\mathbf{R}\in\mathbb{R}^T$, and, thereafter the nonnegativity and integer constraints are treated separately.

The unconstrained and constrained rate allocation problems based on (23) are formulated as follows.

Problem 3: Find the rate allocation $\mathbf{R}$ that solves the problem,

$$\min_{\mathbf{R}}\sum_{t=0}^{T-1}\breve{J}_t(\mathbf{R}_t),\ R_t\in\mathbb{R},\ \forall t,$$

where $\breve{J}_t(\mathbf{R}_t)$ is given by (23).

Problem 4: Find the rate allocation $\mathbf{R}$ that solves the problem,

$$\min_{\mathbf{R}}\sum_{t=0}^{T-1}\breve{J}_t(\mathbf{R}_t),\quad\text{s.t.}\sum_{t=0}^{T-1}R_t\le R_{\mathrm{tot}},\ R_t\in\mathbb{R},\ \forall t,$$

where $\breve{J}_t(\mathbf{R}_t)$ is given by (23).

Next, we present one of the main results of this paper.

Theorem 1:

— For error-free channels ($\epsilon=0$), it holds that a solution $\mathbf{R}\in\mathbb{R}^T$ to

$$\begin{aligned}&\sum_{s=t}^{T-1}\left(2\sum_{b_0=0}^{1}\cdots\sum_{b_t=1}^{1}\cdots\sum_{b_{s-1}=0}^{1}\Psi_s(\mathbf{b}_0^{t-1})\right)=\theta,\ \forall t\\&\qquad\sum_{t=0}^{T-1}R_t=R_{\mathrm{tot}}\end{aligned}\tag{24}$$

solves Problem 4, with θ being the associated Lagrange multiplier, and

$$\begin{aligned}\Psi_t(\mathbf{b}_0^{t-1})\triangleq\pi_t\bar{B}&\left(\prod_{s=\bar{s}+1}^{t-1}\bar{B}_s\right)\\&\times\left(\prod_{m=0}^{t}\tilde{\kappa}_m^{b_m}\right)2^{-2\left(\sum_{n=0}^{t-1}b_nR_n+R_t\right)}.\end{aligned}\tag{25}$$

Here:

1) π_t and $\tilde{\kappa}_t$ are specified in (12) and (17).
2) $\bar{s}$ is the smallest integer s such that $b_s=1$.
3) The term $\bar{B}$ is defined as

$$\bar{B}\triangleq\begin{cases}\tau_{\bar{s}-1}, & \bar{s}>0,\\ B_0\sigma_{x_0}^2, & \bar{s}=0,\end{cases}\tag{26}$$

where B_t is referred to (18), and τ_s is calculated recursively as

$$\tau_s\triangleq A_s\tau_{s-1}+\sigma_v^2,\ \tau_0\triangleq A_0\sigma_{x_0}^2+\sigma_v^2.$$

4) The term $\bar{B}_s$ is chosen between A_s and B_s, determined by b_s,

$$\bar{B}_s\triangleq\begin{cases}A_s, & b_s=0,\\ B_s, & b_s=1.\end{cases}\tag{27}$$

— For noisy channels ($\epsilon\neq0$), it follows that:

1) If $R_{\mathrm{tot}}\ge\sum_{t=0}^{T-1}R_t^\star$, where $\mathbf{R}^\star$ solves

$$\frac{\partial\tilde{\mathrm{J}}_t}{\partial R_t}(\tilde{\beta}_t,\tilde{\kappa}_t,R_t^\star)=0,\ \forall t\tag{28}$$

with $\tilde{\mathrm{J}}_t(\tilde{\beta}_t,\tilde{\kappa}_t,R_t)$ given by (17), then the same $\mathbf{R}^\star$ solves Problem 4.

2) If $R_{\rm tot} < \sum_{t=0}^{T-1} R_t^\star$, where $\mathbf{R}^\star$ is a solution to (28), then the solution to the system of equations

$$-\sum_{s=t}^{T-1} \Psi_{t,s} = \theta,\ \forall t$$
$$\sum_{t=0}^{T-1} R_t = R_{\rm tot} \tag{29}$$

solves Problem 4. Here, the term $\Psi_{t,s}$ is

$$\Psi_{t,s} \triangleq \sum_{b_0=0}^{1} \cdots \sum_{b_t=1}^{1} \cdots \sum_{b_{s-1}=0}^{1} \pi_s \bar{\Psi}(\mathbf{b}_0^s) \tag{30}$$

where $b_k \in \{0,1\}$, $k \in \mathbb{Z}^+$, and

$$\bar{\Psi}(\mathbf{b}_0^s) \triangleq \bar{B}\left(\prod_{m=\bar{s}+1}^{s-1} \bar{B}_m\right)\left(\prod_{n=\bar{s}+1}^{s} C_n^{b_n}\right).$$

The terms $\bar{B}$ and $\bar{B}_n$ are as given by (26)–(27), and C_n is defined as (31)

$$C_n \triangleq \begin{cases} \frac{\partial \tilde{\mathrm{J}}_n}{\partial R_n}(\tilde{\beta}_n, \tilde{\kappa}_n, R_n), & n = t, \\ \tilde{\mathrm{J}}_n(\tilde{\beta}_n, \tilde{\kappa}_n, R_n), & n \neq t. \end{cases} \tag{31}$$

To prove Theorem 1, we use Lemma 2– Lemma 8, as shown subsequently. We start by dealing with the error-free scenario.

A. Error-Free Channels

Lemma 2 presents (23) in a more tractable form.

Lemma 2: Let $\epsilon = 0$. The instantaneous objective function (23) is given by

$$\breve{J}_t(\mathbf{R}_t) = \sum_{b_0=0}^{1} \cdots \sum_{b_{t-1}=0}^{1} \Psi_t(\mathbf{b}_0^{t-1}) \tag{32}$$

where $\Psi_t(\mathbf{b}_0^{t-1})$ is defined in (25).

Proof: For $\epsilon = 0$, the instantaneous objective function (23) is

$$\breve{J}_t(\mathbf{R}_t) = (\phi_{t+1} + \rho)\ell_t^2 \hat{\sigma}_{x_t}^2 \tilde{\kappa}_t 2^{-2R_t} = \pi_t \hat{\sigma}_{x_t}^2 \tilde{\kappa}_t 2^{-2R_t} \tag{33}$$

where $\hat{\sigma}_{x_t}^2 = (A_t + B_t \tilde{\kappa}_t 2^{-2R_{t-1}})\hat{\sigma}_{x_{t-1}}^2 + \sigma_v^2$, with A_t and B_t as given by (18). By recursively replacing $\hat{\sigma}_{x_s}^2$ with $\hat{\sigma}_{x_{s-1}}^2$ and R_{s-1}, for $s = t, \ldots, 1$, up to $\hat{\sigma}_{x_0}^2 = \sigma_{x_0}^2$, then we can write $\hat{\sigma}_{x_t}^2$ as a function of $\mathbf{R}_{t-1}$. In particular, $\breve{J}_t(\mathbf{R}_t)$ is given by a sum of 2^t products, $\Psi_t(\mathbf{b}_0^{t-1})$ from (25), i.e.

$$\Psi_t(\mathbf{b}_0^{t-1}) = \pi_t \bar{B}\left(\prod_{s=\bar{s}+1}^{t-1} \bar{B}_s\right)\left(\prod_{m=0}^{t} \tilde{\kappa}_m^{b_m}\right) 2^{-2\left(\sum_{n=0}^{t-1} b_n R_n + R_t\right)}$$

with all terms described in Theorem 1. ∎

Lemma 3: Consider $\{R_t : 0 \le R_t \le R_t^\star\}$. Then, the overall objective function from Problem 4, i.e.,

$$\sum_{t=0}^{T-1} \breve{J}_t(\mathbf{R}_t) \tag{34}$$

is convex in this region.

Proof: (Sketch) The nontrivial and lengthy proof follows by applying Sylvester's criterion, which requires that all of the principal submatrices of the Hessian have a positive determinant. The determinants can be verified by performing Gaussian elimination and examining the diagonal elements of the resulting triangle matrix. The detailed proof, which we have to remove for lack of space, is given in [43]. ∎

Given a finite $R_{\rm tot}$, the constrained optimization problem can be solved according to Lemma 4.

Lemma 4: Let $\epsilon = 0$. A solution to (24) solves Problem 4.

Proof: We can show that $\frac{\partial \breve{J}_t(\mathbf{R}_t)}{\partial R_s} < 0$ and $\lim_{R_s \to \infty} \frac{\partial \breve{J}_t(\mathbf{R}_t)}{\partial R_s} = 0$, when $\epsilon = 0$. That is to say Problem 3 has a unique global minimum, which is achieved at $R_t^\star = \infty$, $\forall t$. Moreover, the overall objective function is convex, as shown in Lemma 3. Therefore, strong duality holds. When $\epsilon = 0$, the instantaneous objective function (23) becomes $\breve{J}_t(\mathbf{R}_t) = \sum_{b_0=0}^{1} \cdots \sum_{b_{t-1}=0}^{1} \Psi_t(\mathbf{b}_0^{t-1})$, with $\Psi_t(\mathbf{b}_0^{t-1})$ given by (25). Then, we minimize the Lagrangian $\eta(\mathbf{R}, \theta) = \sum_{t=0}^{T-1} \breve{J}_t(\mathbf{R}_t) + \theta\left(\sum_{t=0}^{T-1} R_t - R_{\rm tot}\right)$, with respect to $\{\mathbf{R}, \theta\}$, with θ being the associated Lagrange multiplier. Setting $\frac{\partial \eta(\mathbf{R},\theta)}{\partial \theta} = 0$ and $\frac{\partial \eta(\mathbf{R},\theta)}{\partial R_t} = 0$, $\forall t$, yields immediately (24). ∎

B. Noisy Channels

Moving on to deal with the noisy channel scenario, it should be clear that the approximation $\hat{\sigma}_{x_t}^2$ is essential to the derivation of the overall objective function. Similarly to the error-free scenario, starting at $s = t$, by successively replacing $\hat{\sigma}_{x_s}^2$ with $\hat{\sigma}_{x_{s-1}}^2$, right up to $\hat{\sigma}_{x_0}^2 = \sigma_{x_0}^2$, we can formulate $\hat{\sigma}_{x_t}^2$ as a function of $\mathbf{R}_{t-1}$, $\sigma_{x_0}^2$ and σ_v^2. In particular, $\breve{J}_t(\mathbf{R}_t)$ is a sum of 2^t products, as shown in Lemma 5.

Lemma 5: Let $\epsilon > 0$. The instantaneous objective function (23) can be rewritten as

$$\breve{J}_t(\mathbf{R}_t) = \sum_{b_0=0}^{1} \cdots \sum_{b_{t-1}=0}^{1} \pi_t \Psi_t(\mathbf{b}_0^{t-1}) \tilde{\mathrm{J}}_t(\tilde{\beta}_t, \tilde{\kappa}_t, R_t) \tag{35}$$

where $\tilde{\mathrm{J}}_t(\tilde{\beta}_t, \tilde{\kappa}_t, R_t)$ is as defined in (17), and $\Psi_t(\mathbf{b}_0^{t-1}) \triangleq \bar{B}\left(\prod_{s=\bar{s}+1}^{t-1} \bar{B}_s \left(\tilde{\mathrm{J}}_s(\tilde{\beta}_s, \tilde{\kappa}_s, R_s)\right)^{b_s}\right)$, with π_t, $\bar{B}$, $\bar{B}_s$ given by (12) and(26)–(27), and $\bar{s}$ is the smallest integer s for which $b_s = 1$.

Lemma 5 is proved by straightforward calculation. According to Lemma 5, each $\breve{J}_t(\mathbf{R}_t)$ consists of 2^t terms.

Fig. 4 demonstrates an efficient method to compute the middle term $\Psi_t(\mathbf{b}_0^{t-1})$, where the binary sequence $\mathbf{b}_0^{t-1}$ plays an important role. Note that there are in total 2^t different binary sequences of length t. Each sequence $\mathbf{b}_0^{t-1}$ has a corresponding $\Psi_t(\mathbf{b}_0^{t-1})$, which can be computed by following the binary tree in Fig. 4 from the root to the branch nodes. As a matter of fact, the 2^t branch nodes at the t*th* level represent all the 2^t $\Psi_t(\mathbf{b}_0^{t-1})$ terms. We illustrate the computation of one $\Psi_t(\mathbf{b}_0^{t-1})$ term in Example 2.

Example 2: **Computing** $\Psi_t(0,0,1,1)$ In this example, we demonstrate how to compute $\Psi_t(0,0,1,1)$ by following the binary tree from Fig. 4. Start by setting $s = \sigma_{x_0}^2$, and then successively obtain

$$\begin{aligned} b_0 = 0 &: s := A_0\sigma_0^2 + \sigma_v^2 \\ b_1 = 0 &: s := A_1(A_0\sigma_0^2 + \sigma_v^2) + \sigma_v^2 \\ b_2 = 1 &: s := B_2(A_1(A_0\sigma_0^2 + \sigma_v^2) + \sigma_v^2)\tilde{\mathrm{J}}_2(\tilde{\beta}_2, \tilde{\kappa}_2, R_2) \\ b_3 = 1 &: s := B_3(B_2(A_1(A_0\sigma_0^2 + \sigma_v^2) + \sigma_v^2)\tilde{\mathrm{J}}_2(\tilde{\beta}_2, \tilde{\kappa}_2, R_2)) \\ &\quad \times \tilde{\mathrm{J}}_3(\tilde{\beta}_3, \tilde{\kappa}_3, R_3). \end{aligned}$$

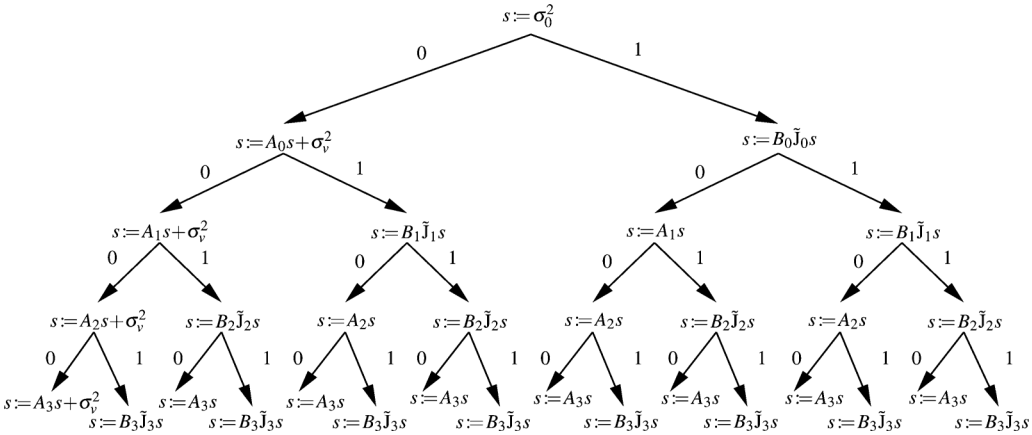

Fig. 4. The breakdown terms of $\Psi_t(\mathbf{b}_0^{t-1})$, where $\tilde{\mathrm{J}}_1$, $\tilde{\mathrm{J}}_2$ and $\tilde{\mathrm{J}}_3$ are short notations for $\tilde{\mathrm{J}}_t(\tilde{\beta}_1, \tilde{\kappa}_1, R_1)$, $\tilde{\mathrm{J}}_t(\tilde{\beta}_2, \tilde{\kappa}_2, R_2)$, and $\tilde{\mathrm{J}}_t(\tilde{\beta}_3, \tilde{\kappa}_3, R_3)$

Finally, $\Psi_t(0,0,1,1) = B_3(B_2(A_1(A_0\sigma_0^2+\sigma_v^2)+\sigma_v^2)\tilde{\mathrm{J}}_2(\tilde{\beta}_2, \tilde{\kappa}_2, R_2))\tilde{\mathrm{J}}_3(\tilde{\beta}_3, \tilde{\kappa}_3, R_3)$.

In Lemma 6, we show the solution to the rate unconstrained problem.

Lemma 6: Let $\epsilon > 0$. Problem 3 has a unique global minimum $\mathbf{R}^\star$, which solves (28).

The proof of Lemma 6 can be found in Appendix I-A.

Lemma 7: Consider $\{R_t : 0 \leq R_t \leq R_t^\star\}$, and the overall objective function (34) from Problem 4 is convex in this region.

Proof: Similar to the proof of Lemma 3, the convexity is also proved by applying Sylvester's criterion, where all of the principal submatrices of the Hessian have a positive determinant. The detailed proof is given in [43]. ∎

Finally, we show how to solve the rate constrained optimization problem, in Lemma 8.

Lemma 8: Let $\epsilon > 0$. A solution to (29) solves Problem 4, where $\Psi_{t,s}$ is given by (30) and θ is the corresponding Lagrangian multiplier.

Proof: The proof is based on Lagrange duality. Strong duality still applies, since the overall objective function has a unique global minimum (Lemma 6), and since the overall objective function is convex in this region (Lemma 7).

Second, we minimize the Lagrangian, $\eta(\mathbf{R},\theta) = \sum_{t=0}^{T-1} \breve{J}_t(\mathbf{R}_t)+\theta(\sum_{t=0}^{T-1} R_t - R_{\mathrm{tot}})$, where $\breve{J}_t(\mathbf{R}_t)$ is given by (42); and θ is the associated Lagrange multiplier. Calculating the derivative $\frac{\partial\eta(\mathbf{R},\theta)}{\partial R_t}$, implies $\frac{\partial\eta(\mathbf{R},\theta)}{\partial R_t} = \sum_{s=t}^{T-1}\Psi_{t,s} + \theta$, where $\Psi_{t,s}$ is given by (30). Note that, all binary variables b_m, $m = 0,\ldots,s$, and $m \neq t$, take both the values of $\{0,1\}$, except b_t, which can only take the value 1. Straightforward calculation shows that the term $\bar{\Psi}(\mathbf{b}_0^s)$ in (30) is

$$\bar{\Psi}(\mathbf{b}_0^s) = \bar{B}\left(\prod_{m=\bar{s}+1}^{s-1}\bar{B}_m\right)\left(\prod_{n=\bar{s}+1}^{s} C_n^{b_n}\right)$$

where the parameters $\bar{B}$ and $\bar{B}_n$ can be found in (26)–(27), and C_n is given by (31). Then, $\frac{\partial\eta(\mathbf{R},\theta)}{\partial R_t} = 0$ and $\frac{\partial\eta(\mathbf{R},\theta)}{\partial\theta} = 0$ lead to (29), which concludes the proof. ∎

We can now give a proof of Theorem 1 by using the previous lemmata:

Proof (Theorem 1): We prove the special case for noiseless channels in three steps. First, we use Lemma 2 to write the overall objective as a function of R_t, $\forall t$, explicitly. Then, we could show that when $\epsilon = 0$, the unconstrained rate allocation problem has a unique global minimum, $R_t^\star = \infty$, $\forall t$. Finally, we use Lemma 3 and Lemma 4 to show that given any $R_{\mathrm{tot}} < \infty$, a solution to (24) solves the constrained rate allocation problem, i.e., Problem 4.

Likewise, we prove the general case for noisy channels also in three steps. First, we use Lemma 5 to write the overall objective as a function of R_t, $\forall t$, explicitly. Then, we use Lemma 6 to show that when $\epsilon > 0$, the unconstrained rate allocation problem has a global minimum which solves (37). This global minimum is the solution to the constrained rate allocation problem if the rate constraint fulfills. Finally, we use Lemma 7 and Lemma 8 to show that the solution to (38) solves the constrained rate allocation problem, if the rate constraint is violated by the global minimum.

This concludes the proof of the theorem. ∎

In the rest of this section, we briefly present the result to the state estimation problem (Problem 2), which is easier to solve compared with Problem 1, i.e., the control counterpart. According to (14), the state x_t is a function of the initial state x_0 and the process noises $\mathbf{v}_0^{t-1}$, namely, $x_t = a^t x_0 + \sum_{s=0}^{t-1} a^{t-1-s} v_s$. Since x_0 and $\mathbf{v}_0^{t-1}$ are i.i.d. zero-mean Gaussian, consequently, x_t is also zero-mean Gaussian with the variance $\sigma_{x_t}^2 = a^{2t}\sigma_{x_0}^2 + \sum_{s=0}^{t-1}(a^{t-1-s})^2\sigma_v^2$. Note that the state x_t does not depend on the communication over the noisy link, and therefore, x_t is not affected by the rate allocation. Hence, the major challenge lies in deriving a useful expression for the MSE, cf., the instantaneous distortion (15). In order to proceed, we resort to approximations based on high rate theory and approximate the distortion (15) by $\hat{\mathrm{J}}_t(\beta_t, \kappa_t, R_t)$ from (16). We thus solve the rate allocation problem with respect to the following average instantaneous distortion:

$$\begin{aligned}\mathbf{E}\left\{J_t(R_t)\right\} &= \hat{\mathrm{J}}_t(\beta_t, \kappa_t, R_t)\\ &= \beta_t(1-(1-\epsilon)^{R_t}) + \kappa_t 2^{-2R_t}. \qquad (36)\end{aligned}$$

The rate unconstrained and constrained optimization problems for state estimation, as an approximate version of Problem 2, are formulated as

Problem 5: Find the rate allocation $\mathbf{R}$ that solves

$$\min_{\mathbf{R}} \sum_{t=0}^{T-1} \hat{\mathrm{J}}_t(\beta_t, \kappa_t, R_t),\ R_t \in \mathbb{R},\ \forall t$$

where $\hat{\mathrm{J}}_t(\beta_t, \kappa_t, R_t)$ is given by (16).

Problem 6: Find the rate allocation $\mathbf{R}$ that solves

$$\min_{\mathbf{R}} \sum_{t=0}^{T-1} \hat{\mathrm{J}}_t(\beta_t, \kappa_t, R_t), \quad \text{s.t.} \sum_{t=0}^{T-1} R_t \leq R_{\text{tot}},\ R_t \in \mathbb{R},\ \forall t$$

where $\hat{\mathrm{J}}_t(\beta_t, \kappa_t, R_t)$ is given by (16).

The solution to Problem 6 is summarized in Theorem 2.

Theorem 2:

- For noisy channels ($\epsilon > 0$)
  1) If $R_{\text{tot}} \geq \sum_{t=0}^{T-1} R_t^\star$, where $\mathbf{R}^\star$ is a solution to
  $$\frac{\partial \hat{\mathrm{J}}_t}{\partial R_t}(\beta_t, \kappa_t, R_t^\star) = 0,\ \forall t \tag{37}$$
  then $\mathbf{R}^\star$ solves Problem 6.
  2) If $R_{\text{tot}} < \sum_{t=0}^{T-1} R_t^\star$, where $\mathbf{R}^\star$ solves (37), then a solution $\{\mathbf{R}, \theta\}$ to
  $$-\frac{\partial \hat{\mathrm{J}}_t}{\partial R_t}(\beta_t, \kappa_t, R_t) = \theta,\ \forall t,\ \sum_{t=0}^{T-1} R_t = R_{\text{tot}} \tag{38}$$
  solves Problem 6, with θ being the associated Lagrange multiplier.
- For error-free channels ($\epsilon = 0$)
$$R_t = \frac{R_{\text{tot}}}{T} + \frac{1}{2}\log_2\left(\frac{\kappa_t}{\left(\prod_{t=0}^{T-1}\kappa_t\right)^{\frac{1}{T}}}\right),\ \forall t \tag{39}$$
solves Problem 6.

To prove Theorem 2, we need Lemma 9–Lemma 11, as shown subsequently.

First, consider the noisy channel scenario, we note that the unconstrained problem for the noisy channel has a unique minimum that is not necessarily achieved at $R_t^\star = \infty$, as stated in Lemma 9.

Lemma 9: Let $\epsilon > 0$. The solution to Problem 5 is a unique global minimum, $\mathbf{R}^\star$, which also solves (37).

Proof: Compute the critical point, at which the gradient of $\sum_{t=0}^{T-1} \hat{\mathrm{J}}_t(\beta_t, \kappa_t, R_t^\star)$ is a zero vector. Straightforward calculation yields (37). It should be remarked that the system of equations is decoupled and the variables $\mathbf{R}$ are separable. We can argue that, since each decoupled function $\hat{\mathrm{J}}_t(\beta_t, \kappa_t, R_t)$ is quasi-convex and has a unique minimum, as shown in Lemma 1, the overall distortion $\sum_{t=0}^{T-1} \hat{\mathrm{J}}_t(\beta_t, \kappa_t, R_t)$ has a unique global minimum. ■

From Lemma 9, we know that if $R_{\text{tot}} \geq \sum_{t=0}^{T-1} R_t^\star$, where $\mathbf{R}^\star$ is a solution to (37), then the same $\mathbf{R}^\star$ also solves Problem 6. On the other hand if $R_{\text{tot}} < \sum_{t=0}^{T-1} R_t^\star$, where $\mathbf{R}^\star$ solves (37), then the solution to (38) solves Problem 6, as stated in the following lemma.

Lemma 10: Let $\epsilon > 0$. The solution to Problem 6 is also a solution to (38).

Proof: The proof is based on Lagrange duality. We note that strong duality holds, because the objective function is a sum of separable quasi-convex functions from Lemma 1, and the constraint is linear. Consider the Lagrangian $\eta(\mathbf{R}, \theta) = \sum_{t=0}^{T-1} \mathbf{E}\{J_t(R_t)\} + \theta(\sum_{t=0}^{T-1} R_t - R_{\text{tot}})$, with θ being the associated Lagrange multiplier. Compute the first-order derivatives of $\eta(\mathbf{R}, \theta)$ with respect to the variables R_t and θ. The minimum is achieved when the derivatives are equal to 0. Observe that, these $T+1$ equations in $T+1$ unknowns, $\mathbf{R}$ and θ, correspond to (38). ■

For an error-free channel ($\epsilon = 0$), the rate allocation problem has a closed-form solution, as shown in Lemma 11.

Lemma 11: Consider Problem 5 where $\epsilon = 0$. A solution $\mathbf{R}$ to (38) is (39).

Proof: Problem 5 is convex and the global minimum is achieved at $R_t^\star = \infty,\ \forall t$. The convexity of the overall objective function $\sum_{t=0}^{T-1} \mathbf{E}\{J_t(R_t)\}$ is readily shown by observing that the Hessian is positive definite. Then, it is straightforward to write R_t as a function of θ, according to (38)

$$\begin{aligned} R_t &= -\frac{1}{2}\log_2\frac{\theta}{2\ln(2)\kappa_t} \\ &= \frac{1}{2}\log_2(2\ln(2)\kappa_t) - \frac{1}{2}\log_2\theta. \end{aligned} \tag{40}$$

We can solve θ by means of the total bit constraint

$$\theta = 2^{\frac{1}{T}\left(\sum_{t=0}^{T-1}\log_2(2\ln(2)\kappa_t) - 2R_{\text{tot}}\right)}. \tag{41}$$

Substituting (41) into (40), (39) follows immediately. ■

The similar results concerning rate allocation in the absence of transmission errors can be found in for example [14]. Finally, we give a brief proof of Theorem 2 by using the previous lemmata.

Proof (Theorem 2): In short, we prove the general case for noisy channels in two steps. We use Lemma 9 to show that when $\epsilon > 0$ the unconstrained rate allocation problem, i.e., Problem 5, has a unique global minimum, which solves (37). This global minimum is the solution to the constrained rate allocation problem, i.e., Problem 6, if the rate constraint fulfills. Then, we use Lemma 10 to show that the solution to (38) solves the constrained rate allocation problem, if the rate constraint is fulfilled.

The special case of noiseless channels is proved in a similar way. This concludes the proof. ■

We remark here that the complexity of the proposed rate allocation method is increasing with time. However, the rate allocation is more relevant for applications with short time horizon. In addition, the computation can be done off-line in advance.

V. Numerical Experiments

In this section, we present numerical experiments to verify the performance of the proposed rate allocation algorithms. Let us first address some issues common for all experiments in this paper. In general, we refer to the rate allocation obtained by applying Theorem 1 as the optimized allocation. In particular, we optimize the rate allocation by means of the objective function (23) of Problem 4, while the overall performance is on the other hand evaluated in term of the objective function (6) of Problem 1. Throughout this section, the initial state and the process noise are zero-mean Gaussian with variances $\sigma_{x_0}^2$ and σ_v^2, respectively. For the exposition of the basic design concept and procedure, we choose to use a time-varying uniform quantizer for which the quantizer range is related to the estimated signal variance as $\vartheta_t = 4\hat{\sigma}_{x_t}$. At the same time, we also use this quantizer to expose the importance of a carefully designed coding-controller. As revealed later, this simple quantizer is far from optimal in view of the efficiency of communications. Moreover, recall that we derived the instantaneous

objective function (23) based on two approximations: First, x_t was assumed to be Gaussian, and, second, we assume that the high-rate form (16) is adopted and the distortion caused by the signals outside the support of the quantizer is negligible. Hence, we use (18) and (22). In this paper, the system of nonlinear (29) is solved numerically using Newton's method. We discuss the validity of these two approximations later in Fig. 8. We deal with the nonnegativity and integer constraints of the rates by using standard rounding approaches, *cf.*, [14] and [44]. In the experiments, we formulate the rounding as a binary optimization problem in which the binary variables represent rounding the rate upwards or downwards to the nearest integer. A solution to such a problem can always be obtained by exhaustive search or combinatorial algorithms [45].

A. Performance of the Rate Allocation Algorithms

First, in Fig. 5(a) we demonstrate the performance of the proposed scheme to the state feedback control problem by comparing it with several other allocations. In many previous works, the transmission rate is constant over time, e.g., [24] and [46]. We show that this is not the most efficient way to utilize the communication resources. The system parameters are chosen in the interest of demonstrating nonuniform rate allocations, in particular, the system setup is: $a = 0.5$, $\rho = 0.1$, $T = 10$, $R_{\text{tot}} = 30$, $\epsilon = 0.001$, $\sigma^2_{x_0} = 10$, and $\sigma^2_v = 0.1$. The simulated costs are obtained by averaging over 100 IA's and for each IA over 150 000 samples. In Fig. 5(a), we compare the optimized allocation, denoted by RA_{12}, which is obtained by the method proposed in this paper, to 13 other allocations, denoted by $RA_1 - RA_{11}$, RA_{13}, and RA_{14}. All 14 allocations are listed in the same figure. Especially, the allocation RA_4 is achieved with our method by solving the unconstrained rate allocation problem. Regarding the optimized allocation, R_t is fairly evenly distributed over t, and compared with the uniform allocation RA_6, there is certain performance improvement. The uniform allocations $RA_1 - RA_8$ have a time-invariant rate from 8 bits to 1 bit. Among these allocations, RA_8, for which $R_t = 1$, $\forall t$, has the worst performance, while RA_4, for which $R_t = 5$, $\forall t$, has the best performance. In fact, based on our analysis, $\tilde{\beta}_t = \tilde{\beta}$, $\tilde{\kappa}_t = \tilde{\kappa}$, and the solution to Problem 3 is $R^\star_t = 5$, $\forall t$. In the presence of channel errors, more bits can sometimes degrade the performance. This is consistent with the simulation result that RA_4 is superior to allocations that are assigned more than 5 bits for every t, *cf.*, $RA_1 - RA_3$. The allocations $RA_9 - RA_{13}$ are used to represent the strategies that more bits are assigned to the initial states. Obviously, this strategy is not efficient in the current example partly because of the following facts. First, as discussed, the additional bits exceeding the critical point do more harm than good. Second, the degradation caused by reducing one bit at a lower rate is much significant than the improvement along with adding one bit at a higher rate. In addition, we in the same figure include the results obtained by using a fixed index assignment, namely the nature binary IA. In this experiment the nature binary IA, in most of cases, yields a lower cost than the random IA. Similar to the random IA, the lowest cost is given by RA_{12}.

In Fig. 5(b), we demonstrate the corresponding simulation results for the state estimation problem. Here, the optimized rate allocation is obtained by applying Theorem 2 and the binary rounding algorithm. The involved system parameters are the same as in Fig. 5(a). Also, the performance for the same 14 allocations, $RA_1 - RA_{14}$ as in Fig. 5(a), are depicted. In particular, RA_4 is still the global optimum which solves the unconstrained optimization problem; while RA_{14} is the optimized rate allocation for state estimation. Performance in Fig. 5(b) is measured by the objective function of Problem 2, and it is obtained by averaging over 100 IA's and each IA 150 000 samples. Compared with the uniform allocation RA_6, we see that our method gives an evident gain. Note that, here RA_{14} outperforms RA_{12}, which is the optimized allocation for state feedback control. An

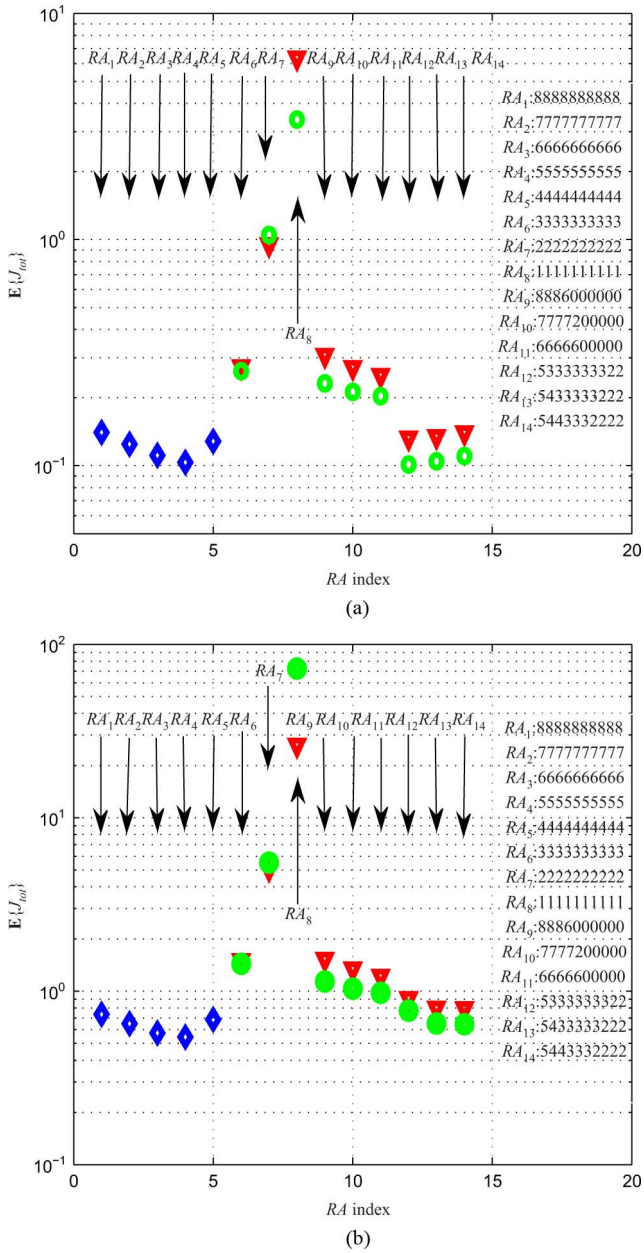

Fig. 5. (a) Performance comparison among various rate allocations for state feedback control. The x axis is associated to the allocation, whereas the y axis is the overall distortion. An allocation is described by an integer vector, for example, RA_{14} has $\mathbf{R} = [5443332222]$. Allocations marked with a diamond do not satisfy the total rate constraint, that is to say $\sum_{t=0}^{T-1} R_t > 30$. Allocations marked with a triangle or a circle fulfill the total rate constraint, $\sum_{t=0}^{T-1} R_t \leq 30$. Allocations marked with a diamond or a triangle use the random IA. Allocations marked with a circle use the nature binary IA. (b) Performance comparison among various rate allocations for state estimation. (a) State feedback control, J_{tot} given by (11). (b) State estimation, J_{tot} given by (15).

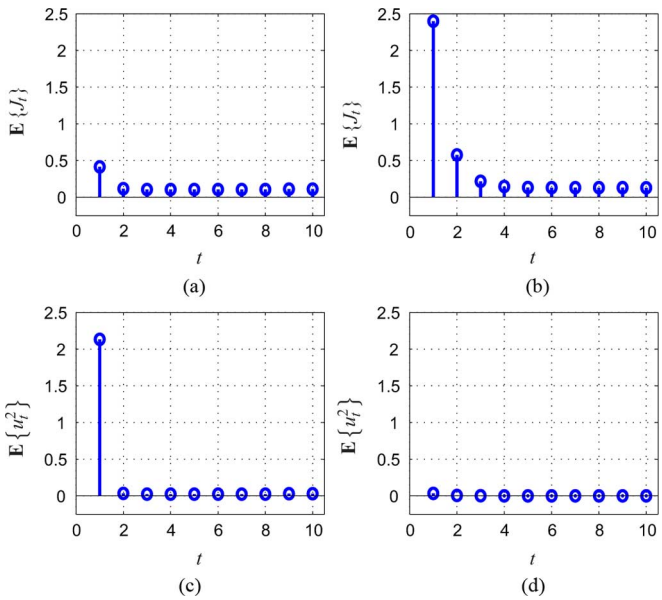

Fig. 6. Performance comparison between $\rho = 0.1$ [(a) and (c)] and $\rho = 10$ [(b) and (d)].

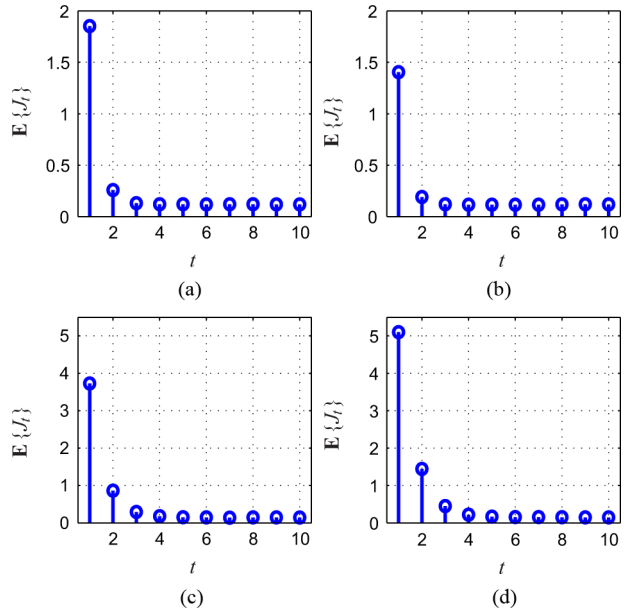

Fig. 7. Performance comparison with respect to epsilon: (a) $\epsilon = 0.001$, RA_7; (b) $\epsilon = 0.001$, RA_{13}; (c) $\epsilon = 0.1$, RA_7; (d) $\epsilon = 0.1$, RA_{13}.

explanation for the gain of RA_{14} is that without control action the trajectory approaches $zero$ slowly which requires more bits in the initial states.

B. Impact of the Weighing Factor ρ

The purpose of this example is to demonstrate the impact of the weighting factor ρ. Recall that ρ plays a role of regulating the power of the control signal. More precisely, the magnitude of the control signal decreases as ρ increases. That is to say, a large ρ yields small-valued controls, consequently, a slow state response and a high steady-state level. In this experiment, we fix the following system parameters, $a = 0.5$, $T = 10$, $R_{\text{tot}} = 30$, $\epsilon = 0.001$, $\sigma_{x_0}^2 = 10$, $\sigma_v^2 = 0.1$, and the aforementioned time-varying uniform quantizer. The optimized rate allocations are $RA_{12} = \{5333333322\}$, $RA_{13} = \{5433333222\}$, $RA_{14} = \{5443322222\}$, for $\rho = 0.1,\ 1,\ 10$, respectively. By applying Lemma 6, we see that the global minimum to the rate unconstrained problem is $R_t^\star = R^\star = 5$. This is consistent with the above derived rate allocations that there is no R_t larger than 5. When ρ is small, for example $\rho = 0.1$, large-valued controls are allowed and the steady state is quickly reached. As ρ increases, only small-valued controls are allowed and it takes longer time to reach the steady state. This explains RA_{14} that more bits are needed in the initial states when ρ is large. As mentioned previously, the rate allocation RA_{14} is also the solution to the state estimation problem. Interestingly, the optimized rate allocation in this case is the same as when $\rho = 10$. It is a reasonable observation, since, when $\rho = 10$, first, the controls are extremely small and have hardly impact on the state evolution; second, π_t is nearly constant. As a result, Problem 4 becomes similar to the estimation problem, cf., Theorem 2. The simulated instantaneous costs for $\rho = 0.1$ and $\rho = 10$ are depicted in Fig. 6. Indeed, the instantaneous cost for $\rho = 10$ is remarkably higher than the one for $\rho = 0.1$, because the former system performs similarly to the one without any control.

C. Impact of the Cross-Over Probability ε

The impact of the cross-over probability ϵ is studied in Fig. 7, where we fix the other parameters and only vary ϵ. As before, the system setup is: $T = 10$, $R_{\text{tot}} = 30$, $\rho = 1$, $\sigma_{x_0}^2 = 10$ and $\sigma_v^2 = 0.1$. Applying Theorem 1, we obtain RA_{13} for $\epsilon = 0.001$, and RA_7 for $\epsilon = 0.1$, respectively. At $\epsilon = 0.001$, the global minimum to the unconstrained problem, according to Lemma 6, is $R_t^\star = 5$, which means the rate constraint is violated at the global minimum. On the other hand, at $\epsilon = 0.1$, the global minimum is $R_t = 2$, so the rate constraint applies. Since the quantizer range is fixed, a reduction in the rate causes a higher quantization error, but more robust codewords against transmission errors. Beyond a certain number, the "additional bits" will do more harm than good, as demonstrated in Fig. 7. In the figure, the simulated instantaneous costs obtained by using RA_{13} and RA_7 at $\epsilon = 0.001$ and $\epsilon = 0.1$, are depicted. At $\epsilon = 0.001$, if $R_t > 5$, we can improve the performance by increasing the rate. Therefore, RA_{13} outperforms RA_7. At $\epsilon = 0.1$, the situation is different. When $R_t > 2$, the performance is degraded by increasing the rate, which is consistent to the simulation result in Fig. 7.

D. Additional Remarks

We conclude this section by some additional remarks. In Section II, we have formulated Problem 1 to assign totally R_{tot} bits optimally to T time units. In fact, the solutions to the optimal rate allocation problem have partly answered the question the other way round. That is to say how much data it is truly needed to achieve a certain system behavior. In the absence of channel errors, increasing the data rate typically means more accurate information, consequently, a better control performance. Unfortunately, in the presence of channel errors, the situation is complicated. The channel error has different kinds of impact on the system performance. First, if the encoder-controller is not optimal, increasing the data rate does not necessarily improve the performance. Moreover, the improvement given by the rate is significantly reduced if ϵ is

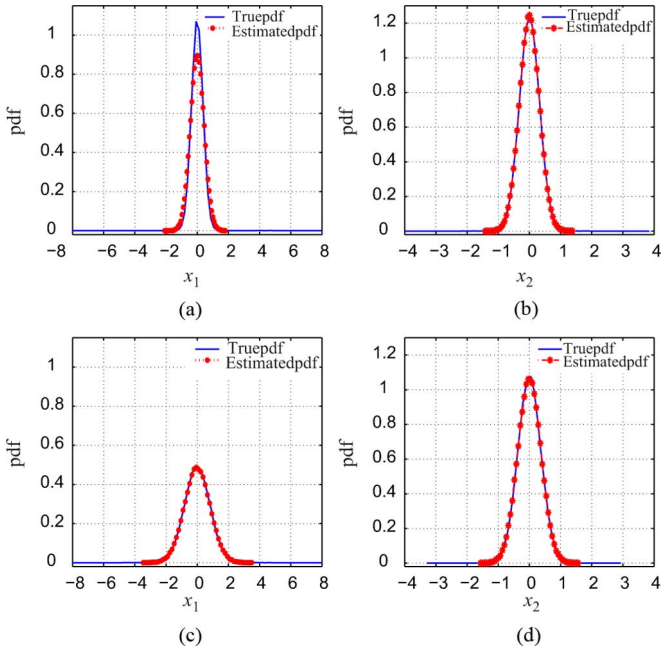

Fig. 8. The pdf's of the estimated x_t and the true $x_t, t = 1, 2$, for two ρ values.

high. It is worth noticing that the solution to the unconstrained problem can be used to evaluate the optimality of the quantizer. In particular, optimal quantizers will solve Problem 3 with $R^\star = \infty$. In other words, by optimizing the encoder-decoder pair, we can move $R^\star$ towards ∞ to enhance the efficiency of the available communication resources.

Finally, we would like to make a few comments on the accuracy of the approximations (the high-rate approximation and the Gaussian state approximation). Regarding the high-rate approximation of the MSE, although the high-rate assumption requires the source pdf to be approximately constant over one quantization cell, the high-rate approximation works fairly well in practice for as low rates such as 3, 4 bits. On the other hand, we may say generally that the accuracy decreases when the rate approaches 0. The worst case occurs at $R_t = 0$, where the estimation error $\mathbf{E}\left\{(x_t - d_t)^2\right\}$ given by (16) is even worse than σ_x^2, obtained by setting $d_t = 0$. Finally, the Gaussian approximation becomes less accurate as the significance of control increases, which is assessed below by a numerical example. In Fig. 8, a comparison of the pdf's of the estimated x_t and the true x_t is depicted, for two ρ values: $\rho = 0.1$ and $\rho = 1$. The other parameters retain the same values, i.e., $a = 0.5$, $T = 10$, $R_{\text{tot}} = 30$, $\epsilon = 0.001$, $\sigma_{x_0}^2 = 10$, $\sigma_v^2 = 0.1$. We could observe that for large-valued ρ, the influence of control is moderate. Consequently, the system behaved more like the open-loop system. Therefore the Gaussian assumption is more accurate. On the other hand, for small-valued ρ, the influence of control is significant, which reduces slightly the accuracy of the Gaussian assumption of the state x_t. We conclude that the assumption works well in practice.

VI. Conclusion

We proposed a new method to optimize the allocation of communication resources in state feedback control and state estimation over noisy channels. More specifically, we studied the problem of optimal rate allocation with control and/or estimation performance as the utility function. In order to arrive at a tractable objective function, we first approximated the objective functions by means of the high-rate approximation theory. Second, for each rate allocation problem, we showed that the unconstrained version has a global minimum, which solves the problem if such a global minimum does not violate the rate constraint. On the other hand, if the global minimum violates the rate constraint, then we solved the rate constrained optimization problems by means of Lagrangian duality. Numerical simulations showed good performance of the proposed method and that, contrarily to previous studies, it is better to give an unequal rate allocation.

Future work include the extension of our rate allocation scheme to handle networked control systems of multiple plants. For example in the presence of a shared communication medium, a total transmission rate constraint could be imposed to formulate optimization problems of multi-objective utility functions. Meanwhile, it is also interesting to investigate how the interference between the plants can affect the rate allocation.

Appendix

Proof of Lemma 6: According to Lemma 5, $\breve{J}_t(\mathbf{R}_t)$ can be written as

$$\breve{J}_t(\mathbf{R}_t) = \sum_{b_0=0}^{1} \cdots \sum_{b_{t-1}=0}^{1} W(\mathbf{b}_0^{t-1}) \prod_{s=0}^{t-1} \left(\tilde{\mathrm{J}}_s(\tilde{\beta}_s, \tilde{\kappa}_s, R_s)\right)^{b_s} \tilde{\mathrm{J}}_t(\tilde{\beta}_t, \tilde{\kappa}_t, R_t). \quad (42)$$

The coefficient $W(\mathbf{b}_0^{t-1}) \triangleq \pi_t \bar{B} \left(\prod_{s=\bar{s}+1}^{t-1} \bar{B}_s\right)$ is independent of $\mathbf{R}_{t-1}$, and the parameters π_t, $\bar{B}$, $\bar{B}_s$ and $\bar{s}$ are given in Theorem 1. Taking the first-order derivative of $\breve{J}_t(\mathbf{R}_t)$ gives

$$\frac{\partial}{\partial R_k}\breve{J}_t(\mathbf{R}_t) = \frac{\partial \tilde{\mathrm{J}}_k}{\partial R_k}(\tilde{\beta}_k, \tilde{\kappa}_k, R_k) \left(\sum_{b_0=0}^{1} \cdots \sum_{b_k=1}^{1} \cdots \sum_{b_{t-1}=0}^{1} W(\mathbf{b}_0^{t-1}) \times \prod_{\substack{s=0 \\ s\neq k}}^{t-1} \left(\tilde{\mathrm{J}}_s(\tilde{\beta}_s, \tilde{\kappa}_s, R_s)\right)^{b_s} \tilde{\mathrm{J}}_t(\tilde{\beta}_t, \tilde{\kappa}_t, R_t) \right), \; k < t$$

$$\frac{\partial}{\partial R_t}\breve{J}_t(\mathbf{R}_t) = \frac{\partial \tilde{\mathrm{J}}_t}{\partial R_t}(\tilde{\beta}_t, \tilde{\kappa}_t, R_t) \left(\sum_{b_0=0}^{1} \cdots \sum_{b_{t-1}=0}^{1} W(\mathbf{b}_0^{t-1}) \times \prod_{s=0}^{t-1} \left(\tilde{\mathrm{J}}_s(\tilde{\beta}_s, \tilde{\kappa}_s, R_s)\right)^{b_s} \right), \quad (43)$$

where the sums are positive. Note that $\frac{\partial \breve{J}_t(\mathbf{R}_t)}{\partial R_k} = 0$, for $k > t$. Since (43) applies for all t, it follows that at the critical point $\frac{\partial}{\partial R_k}\sum_{t=0}^{T-1} \breve{J}_t(\mathbf{R}_t) = 0$, so that $\frac{\partial \tilde{\mathrm{J}}_k}{\partial R_k}(\tilde{\beta}_k, \tilde{\kappa}_k, R_k^\star) = 0$. Computing the second-order derivatives, implies

$$\frac{\partial^2 \breve{J}_t(\mathbf{R}_t)}{\partial R_k^2} = \frac{\partial^2 \tilde{\mathrm{J}}_k}{\partial R_k^2}(\tilde{\beta}_k, \tilde{\kappa}_k, R_k) \left(\sum_{b_0=0}^{1} \cdots \sum_{b_k=1}^{1} \cdots \sum_{b_{t-1}=0}^{1} W(\mathbf{b}_0^{t-1}) \times \prod_{\substack{s=0 \\ s\neq k}}^{t-1} \left(\tilde{\mathrm{J}}_s(\tilde{\beta}_s, \tilde{\kappa}_s, R_s)\right)^{b_s} \tilde{\mathrm{J}}_t(\tilde{\beta}_t, \tilde{\kappa}_t, R_t) \right), \; k < t,$$

$$\frac{\partial^2 \breve{\mathrm{J}}_t(\mathbf{R}_t)}{\partial R_k \partial R_l} = \frac{\partial \tilde{\mathrm{J}}_k}{\partial R_k}(\tilde{\beta}_k, \tilde{\kappa}_k, R_k) \frac{\partial \tilde{\mathrm{J}}_l}{\partial R_l}(\tilde{\beta}_l, \tilde{\kappa}_l, R_l) \left(\sum_{b_0=0}^{1} \cdots \sum_{b_k=1}^{1} \sum_{b_l=1}^{1} \cdots \sum_{b_{t-1}=0}^{1} W(\mathbf{b}_0^{t-1}) \prod_{\substack{s=0 \\ s\neq k,l}}^{t-1} \left(\tilde{\mathrm{J}}_s(\tilde{\beta}_s, \tilde{\kappa}_s, R_s) \right)^{b_s} \right) \times \tilde{\mathrm{J}}_t(\tilde{\beta}_t, \tilde{\kappa}_t, R_t), \quad k, l < t, \quad k \neq l$$

$$\frac{\partial^2 \breve{\mathrm{J}}_t(\mathbf{R}_t)}{\partial R_t^2} = \frac{\partial^2 \tilde{\mathrm{J}}_t}{\partial R_t^2}(\tilde{\beta}_t, \tilde{\kappa}_t, R_t) \left(\sum_{b_0=0}^{1} \cdots \sum_{b_{t-1}=0}^{1} \times W(\mathbf{b}_0^{t-1}) \prod_{s=0}^{t-1} \left(\tilde{\mathrm{J}}_s(\tilde{\beta}_s, \tilde{\kappa}_s, R_s) \right)^{b_s} \right),$$

$$\frac{\partial^2 \breve{\mathrm{J}}_t(\mathbf{R}_t)}{\partial R_t \partial R_l} = \frac{\partial \tilde{\mathrm{J}}_t}{\partial R_t}(\tilde{\beta}_t, \tilde{\kappa}_t, R_t) \frac{\partial \tilde{\mathrm{J}}_l}{\partial R_l}(\tilde{\beta}_l, \tilde{\kappa}_l, R_l) \times \left(\sum_{b_0=0}^{1} \cdots \sum_{b_l=1}^{1} \cdots \sum_{b_{t-1}=0}^{1} W(\mathbf{b}_0^{t-1}) \prod_{\substack{s=0 \\ s\neq l}}^{t-1} \left(\tilde{\mathrm{J}}_s(\tilde{\beta}_s, \tilde{\kappa}_s, R_s) \right)^{b_s} \right) \quad l < t.$$

Note that if k or $l > t$, the second-order derivative is 0. At the critical point, $\frac{\partial \tilde{\mathrm{J}}_k}{\partial R_k} = 0$ and $\frac{\partial^2 \tilde{\mathrm{J}}_k}{\partial R_k^2} > 0$, hence, all elements at the diagonal of the Hessian matrix are positive. We can conclude that the Hessian matrix is positive definite and the critical point is a global minimum.

ACKNOWLEDGMENT

The authors would like to thank the associate editor and the anonymous reviewers for many very helpful comments that considerably helped to improve the quality of the paper.

REFERENCES

[1] Z.-Q. Luo, M. Gastpar, J. Liu, and A. Swami, "Distributed signal processing in sensor networks," *IEEE Signal Process. Mag.*, vol. 23, no. 4, 2006.

[2] A. Willig, "Recent and emerging topics in wireless industrial communication," *IEEE Trans. Indust. Inf.*, vol. 4, no. 2, pp. 102–124, 2008.

[3] S. Verdú, "Spectral efficiency in the wideband regime," *IEEE Trans. Inf. Theory*, vol. 48, no. 6, pp. 1319–1343, 2002.

[4] M. Sabin and R. Gray, "Global convergence and empirical consistency of the generalized Lloyd algorithm," *IEEE Trans. Inf. Theory*, vol. 32, no. 2, pp. 148–155, Mar. 1986.

[5] S. Tatikonda, A. Sahai, and S. Mitter, "Stochastic linear control over a communication channel," *IEEE Trans. Autom. Control*, vol. 49, no. 9, pp. 1549–1561, Sep. 2004.

[6] L. Bao, M. Skoglund, and K. H. Johansson, "Iterative encoder-controller design for feedback control over noisy channels," *IEEE Trans. Autom. Control*, vol. 56, no. 2, pp. 256–278, Feb. 2011.

[7] F. Meshkati, H. V. Poor, and S. C. Schwartz, "Energy-efficient resource allocation in wireless networks," *IEEE Signal Process. Mag.*, vol. 24, no. 3, pp. 58–68, 2007.

[8] X. Wang, A. G. Marques, and G. B. Giannakis, "Power-efficient resource allocation and quantization for TDMA using adaptive transmission and limited-Rate feedback," *IEEE Trans. Signal Process.*, vol. 56, no. 9, pp. 4470–4485, Sep. 2008.

[9] R. Zhang, Y.-C. Liang, and S. Cui, "Dynamic resource allocation in cognitive radio networks," *IEEE Signal Process. Mag.*, vol. 27, no. 3, pp. 102–114, 2010.

[10] F. Chen, W. Su, S. Batalama, and J. D. Matyjas, "Joint power optimization for multi-source multi-destination relay networks," *IEEE Trans. Signal Process.*, vol. 59, no. 5, pp. 2370–2381, 2011.

[11] P. C. Weeraddana, M. Codreanu, M. Latva-aho, and A. Ephremides, "Resource allocation for cross-layer utility maximization in wireless networks," *IEEE Trans. Veh. Technol.*, vol. 60, no. 6, pp. 2790–2809, 2011.

[12] Q. Ling and M. D. Lemmon, "Stability of quantized control systems under dynamic bit assignment," *IEEE Trans. Autom. Control*, vol. 50, no. 5, pp. 734–740, 2005.

[13] L. Xiao, M. Johansson, H. Hindi, S. Boyd, and A. Goldsmith, "Joint optimization of wireless communication and networked control systems," *Chap. Switching Learn., Springer Lecture Notes in Comput. Sci. 3355*, vol. 32, no. 2, pp. 148–155, Mar. 1986.

[14] A. Gersho and R. M. Gray, *Vector Quantization and Signal Compression*. New York: Kluwer, 1992.

[15] B. Farber and K. Zeger, "Quantization of multiple sources using nonnegative integer bit allocation," *IEEE Trans. Inf. Theory*, vol. 52, no. 11, pp. 4945–4964, 2006.

[16] S. W. Mclaughlin and D. L. Neuhoff, "Asymptotic quantization for noisy channels," in *Proc. IEEE Int. Symp. Inf. Theory*, 1993, p. 442.

[17] R. Gupta and A. O. Hero, "High-rate vector quantization for detection," *IEEE Trans. Inf. Theory*, vol. 49, no. 8, pp. 1951–1969, Aug. 2003.

[18] C. R. Murthy and B. D. Rao, "High-rate analysis of source coding for symmetric error channels," in *Proc. IEEE Data Compress. Conf. (DCC)*, 2006, pp. 163–172.

[19] N. Farvardin and J. W. Modestino, "Optimum quantizer performance for a class of non-Gaussian memoryless sources," *IEEE Trans. Inf. Theory*, vol. 30, no. 3, pp. 485–497, May 1984.

[20] J. Lim, "Optimal bit allocation for noisy channels," *Electron. Lett.*, vol. 41, no. 7, pp. 405–406, Mar. 2005.

[21] B. Widrow, "Statistical analysis of amplitude-quantized sampled-data systems," *Amer. Inst. Elect. Eng., Pt.II (Appl. Ind.)*, pp. 555–568, 1961.

[22] D. F. Delchamps, "Stabilizing a linear system with quantized state feedback," *IEEE Trans. Autom. Control*, vol. 35, no. 8, pp. 916–924, Aug. 1990.

[23] F. Fagnani and S. Zampieri, "Stability analysis and synthesis for scalar linear systems with a quantized feedback," *IEEE Trans. Autom. Control*, vol. 48, no. 9, pp. 1569–1584, Sep. 2003.

[24] S. Tatikonda and S. Mitter, "Control under communication constraints," *IEEE Trans. Autom. Control*, vol. 49, no. 7, pp. 1056–1068, Jul. 2004.

[25] D. Liberzon, "Stabilization by quantized state or output feedback: a hybrid control approach," *Proc. IFAC 15th Triennial World Congr.*, pp. 79–84, 2002.

[26] A. V. Savkin, "Analysis and synthesis of networked control systems: topological entropy, observability, robustness and optimal control," *Automatica*, vol. 42, pp. 51–62, 2006.

[27] S. Yüksel and T. Basar, "Minimum rate coding for LTI systems over noiseless channels," *IEEE Trans. Autom. Control*, vol. 51, no. 12, pp. 1878–1887, 2006.

[28] G. N. Nair, F. Fagnani, S. Zampieri, and R. Evans, "Feedback control under data rate constraints: an overview," *Proc. IEEE*, pp. 108–137, Jan. 2007.

[29] A. Sahai and S. Mitter, "The necessity and sufficiency of anytime capacity for stabilization of a linear system over a noisy communication link—part I: Scalar systems," *IEEE Trans. Inf. Theory*, vol. 52, no. 8, pp. 3369–3395, 2006.

[30] J. P. Hespanha, P. Naghshtabrizi, and Y. Xu, "A survey of recent results in networked control systems," *Proc. IEEE*, vol. 95, no. 1, pp. 138–162, Jan. 2007.

[31] C. D. Charalambous and A. Farhadi, "LQG optimality and separation principle for general discrete time partially observed stochastic systems over finite capacity communication channels," *Automatica*, vol. 44, pp. 3181–3188, 2008.

[32] S. Tatikonda and S. Mitter, "The capacity of channels with feedback," *IEEE Trans. Inf. Theory*, vol. 55, no. 1, pp. 323–349, 2009.

[33] E. I. Silva, J. Østergaard, and M. Derpich, "On the minimal average data-rate that guarantees a given closed loop performance level," in *Proc. 2nd IFAC Workshop on Estimation and Contr. Netw. Syst. (NecSys)*, 2010.

[34] P. Antsaklis and J. Baillieul, "Special issue on technology of networked control systems," *Proc. IEEE*, vol. 95, no. 1, pp. 5–8, Jan. 2007.

[35] R. A. Gupta and M. Y. Chow, "Networked control systems: Overview and research trends," *IEEE Trans. Indust. Electron.*, vol. 57, no. 7, pp. 2527–2535, 2010.

[36] L. Bao, M. Skoglund, C. Fischione, and K. H. Johansson, "rate allocation for quantized control over binary symmetric channels" (full version) Royal Inst. Technol., Stockholm, Sweden, Tech. Rep. IR/EE/2011:054, 2011.

[37] N. Farvardin, "A study of vector quantization for noisy channels," *IEEE Trans. Inf. Theory*, vol. 36, no. 4, pp. 799–809, 1990.
[38] K. Zeger and V. Manzella, "Asymptotic bounds on optimal noisy channel quantization via random coding," *IEEE Trans. Inf. Theory*, vol. 40, no. 6, pp. 1926–1938, Nov. 1994.
[39] R. G. Gallager, *Information Theory and Reliable Communication*. New York: Wiley, 1968.
[40] S. Boyd and L. Vandenberghe, *Convex Optimization*. Cambridge, U.K.: Cambridge Univ. Press, 2004.
[41] M. Chiang, *Geometric Programming for Communication Systems, Foundations and Trends in Communications and Information Theory*. New York: Now, 2005.
[42] M. Aoki, *Optimization of Stochastic Systems—Topics in Discrete-Time Systems*. New York: Academic, 1967.
[43] L. Bao, M. Skoglund, C. Fischione, and M. Skoglund, "On rate allocation for multiple plants in a networked control system," in *Proc. Amer. Control Conf. (ACC)*, 2012.
[44] B. Farber and K. Zeger, "Quantization of multiple sources using integer bit allocation," in *Proc. IEEE Data Compress. Conf.*, 2005, pp. 368–377.
[45] C. H. Papadimitriou and K. Steiglitz, *Combinatorial Optimization: Algorithms and Complexity*. New York: Dover, 1998.
[46] R. W. Brockett and D. Liberzon, "Quantized feedback stabilization of linear systems," *IEEE Trans. Autom. Control*, vol. 45, no. 7, pp. 1279–1289, Jul. 2000.

Lei Bao (S'04–M'09) received the M.Sc. degree in electrical engineering with specialization in digital communication from Chalmers university of Technology, Gothenburg, Sweden, in 2003, and the Ph.D. degree in telecommunication from the Royal Institute of Technology (KTH), Stockholm, Sweden, in 2009.

She is currently with Ericsson Research. Her research interests include communication theory and coding theory for networked control.

Mikael Skoglund (S'93–M'97–SM'04) received the Ph.D. degree in 1997 from Chalmers University of Technology, Sweden. In 1997, he joined the Royal Institute of Technology (KTH), Stockholm, Sweden.

He was appointed to the Chair in Communication Theory in 2003 at KTH, where he heads the Communication Theory Lab and is also the Assistant Dean for Electrical Engineering. His research interests are in the theoretical aspects of wireless communications. He has worked on problems in source-channel coding, coding and transmission for wireless communications, Shannon theory, and statistical signal processing. He has authored and coauthored almost 300 scientific papers. He has also consulted for industry, and he holds six patents.

Dr. Skoglund has served on numerous Technical Program Committees for IEEE conferences. During 2003–2008, he was an Associate Editor with the IEEE TRANSACTIONS ON COMMUNICATIONS. He is presently on the editorial board for IEEE TRANSACTIONS ON INFORMATION THEORY. He has authored many papers that have received awards, invited conference presentations, and papers ranking as highly cited according to the ISI Essential Science Indicators.

Carlo Fischione (M'02) received the Ph.D. degree in electrical and information engineering in May 2005 from the University of L'Aquila, Italy, and the Dr.Eng. degree in electronic engineering (Laurea, *summa cum laude*, 5/5 years) in April 2001 from the same University.

He is a tenured Associate Professor with the Electrical Engineering and ACCESS Linnaeus Center, Automatic Control Lab, KTH Royal Institute of Technology, Stockholm, Sweden. He held research positions at the University of California at Berkeley (2004–2005 and 2007–2008) and the KTH (2005–2007). His research interests include optimization, wireless sensor networks, networked control systems, and system level design of wireless networks. He has coauthored more than 70 publications in international journals and conferences and an international patent.

Dr. Fischione received the Best Paper award from the IEEE TRANSACTIONS ON INDUSTRIAL INFORMATICS of 2007, the Best Paper awards at the IEEE International Conference on Mobile *Ad-hoc* and Sensor System '05 and '09 (IEEE MASS 2005 and IEEE MASS 2009), the Best Business Idea Award from VentureCup East Sweden 2010, the "Ferdinando Filauro" Award from the University of L'Aquila, and the "Higher Education" Award from the Abruzzo Region Government, Italy. In 2008 he received an Individual Junior Research Grant from the Swedish Research Council. He has chaired or served as a Technical Member of Program Committees of several international conferences and is serving as referee for technical journals. Meanwhile, he also has offered his advice as a consultant to numerous technology companies such as Berkeley Wireless Sensor Network Lab, Ericsson Research, Synopsys, and United Technology Research Center. He is member of the Society for Industrial and Applied Mathematics (SIAM) and ordinary member of DASP (academy of history Deputazione Abruzzese di Storia Patria).

Karl Henrik Johansson (SM'08) received the M.Sc. and Ph.D. degrees in electrical engineering from Lund University, Sweden.

He is Director of the ACCESS Linnaeus Centre and Professor at the School of Electrical Engineering, Royal Institute of Technology, Stockholm, Sweden. He is a Wallenberg Scholar and has held a Senior Researcher Position with the Swedish Research Council. He has held visiting positions at University of California at Berkeley (1998–2000) and the California Institute of Technology, Pasadena (2006–207). His research interests are in networked control systems, hybrid and embedded control, and control applications in automation, communication, and transportation systems.

Dr. Johansson was a member of the IEEE Control Systems Society Board of Governors 2009 and Chair of the IFAC Technical Committee on Networked Systems 2008–2011. He has been on the Editorial Boards of the IEEE TRANSACTIONS ON AUTOMATIC CONTROl and the IFAC journal *Automatica*. He is currently on the Editorial Boards of IET *Control Theory and Applications* and the *International Journal of Robust and Nonlinear Control*. He was the General Chair of the ACM/IEEE Cyber-Physical Systems Week (CPSWEEK) 2010 in Stockholm. He has served on the Executive Committees of several European and national research projects in the area of networked embedded systems. He was awarded an Individual Grant for the Advancement of Research Leaders from the Swedish Foundation for Strategic Research in 2005. He received the triennial Young Author Prize from IFAC in 1996 and the Peccei Award from the International Institute of System Analysis, Austria, in 1993. He received Young Researcher Awards from Scania in 1996 and from Ericsson in 1998 and 1999.